STUDY OF THE IMPACT OF NONLINEARITIES ON ADVANCED MODULATION FORMATS IN OPTICAL SYSTEMS AND NETWORKS

by

Yi-Ping Wang

A Thesis Submitted to the Faculty of the

COLLEGE OF OPTICAL SCIENCES

In Partial Fulfillment of the Requirements

For the Degree of

MASTER OF SCIENCE

In the Graduate College

THE UNIVERSITY OF ARIZONA

2017

STATEMENT BY AUTHOR

The thesis titled STUDY OF THE IMPACT OF NONLINEARITIES ON ADVANCED MODULATION FORMATS IN OPTICAL SYSTEMS AND NETWORKS prepared by Yi-Ping Wang has been submitted in partial fulfillment of requirements for a master's degree at the University of Arizona and is deposited in the University Library to be made available to borrowers under rules of the Library.

Brief quotations from this thesis are allowable without special permission, provided that an accurate acknowledgement of the source is made. Requests for permission for extended quotation from or reproduction of this manuscript in whole or in part may be granted by the head of the major department or the Dean of the Graduate College when in his or her judgment the proposed use of the material is in the interests of scholarship. In all other instances, however, permission must be obtained from the author.

SIGNED: Yi-Ping Wang

APPROVAL BY THESIS DIRECTOR

This thesis has been approved on the date shown below:

MILORAD CVIJETIC
Prof. of Optical Science

Thesis Director Name
Job title (e.g. Professor of Chemistry)

12/06/2017

Date
(Defense date)

Contents

Lists of Figures

Abstract

Chromatic dispersion, Kerr nonlinearity, and amplified spontaneous emission (ASE) noise are three common problems for the optical communication systems. For the systems using direct detection scheme, we detect the power of the signal. Therefore, the information is carried by the signal power, which is pulse amplitude modulation (PAM). In this system, chromatic dispersion and Kerr nonlinearity will broaden the pulse and cause intersymbol interference, while ASE noise will degrade the signal to noise ratio and increase the error rate. For the system using coherent detection, we can detect not only the power but also the phase of the signal. Thus, the information can be carried by the power and the phase of the signal, which is quadrature amplitude modulation (QAM). In this system, the signal will see a phase shift during the propagation induced by the Kerr nonlinearity, which will cause an error if the phase shift is not corrected on the receiver side. In order to optimize the performance or design the solution for the system, a careful study of the impact of these three effects on the signal is needed. In this thesis, I study the theory of the pulse broadening effect caused by chromatic dispersion and Kerr nonlinearity, and as well as the bit error rate performance with the accumulation of ASE noise. Moreover, I use split-step Fourier method to solve the nonlinear Schrödinger equation in MATLAB and simulate the propagation of 2-PAM and 4-QAM signal. The impact of these three effects and the bit error rate behavior of the coherent detection system are demonstrated and discussed.

Chapter 1

Introduction

Nowadays, the requirement of the information transmission rate becomes very large. More people use the internet to connect with others all over the world, which means that we need to transmit more data at the same time and extend the transmission length. Due to the low loss property of fiber, people start to use optical fiber as the information transmission media after Corning introduced the low attenuation fiber. Therefore, it is important to know what happens when the light signal propagates in the fiber and how to increase the transmission rate in the fiber.

Since the optical communication began in 1966 [1], people have developed many techniques to increase the data transfer rate. In the very beginning, people use on-off keying (OOK) to modulate the light source and send the zero-one bit data [2]. Later on, the detection technique is improved, people start to use multilevel pulse amplitude modulation (M-PAM) [3], which increase the number of bits represented by one symbol. For example, if the modulated signal has four amplitude level, then one received symbol (pulse) can stand for two bits (level one stand for 00; level two stand for 01, the rest stand for 10 and 11). Since the coherent detection is used [4], we can detect the phase of the signal, not only the power. Thus, modulation formats like phase shift keying (PSK) is introduced. This modulation format can reduce the power consumption compared to the PAM format because the information is carried on the phase of the light but not by the

amplitude of the pulse. For example, we can use a pulse with same amplitude, and four different phase $0, \frac{\pi}{2}, \pi, \frac{3\pi}{2}$ to represent two bits at a time just like 4-PAM signal. Finally, the hybrid of the PAM and PSK become quadrature amplitude modulation (QAM) format [5, 6], which use two orthogonal basis function $\cos(\omega t)$ and $\sin(\omega t)$ to carry the information. These are the modulation techniques people use to increase the bit rate of the single optical channel (single wavelength). On the other hand, there are some multiplexing techniques that can increase the number of the optical channels that can propagate in the fiber simultaneously, such as polarization-division multiplexing (PDM) [7, 8]: two optical channels with orthogonal polarization states propagate at the same time, space-division multiplexing (SDM) [9]: multiple optical channels with different orbital angular momentum (OAM) states, and orthogonal frequency division multiplexing (OFDM) [10-12]: multiple channels with different carrier frequencies that are orthogonal in the frequency domain. In this thesis, we will focus on the PAM and QAM modulation technique, analyze the transmission property of the system and the performance of the PAM and QAM signal quality. In Chapter 2, we will introduce the theoretical principle of the optical communication system, including three main problems we face when the optical signal propagating in the fiber, how we deal with them, and how these problems affect the transmission quality. In Chapter 3, we use numerical methods to simulate the behavior of the optical signal propagating in the communication system. We will introduce the numerical method we use and the process of simulation. In the end, we compare the simulation result and theoretical study and then have some discussion about the difference between them.

Chapter 2

Principles of optical communication systems

When we talk about the optical communication systems, we usually use achievable bit rate (how many bits we can send per second) [13], propagation length [14, 15], and bit error rate (BER, ratio between error bit and transmitted bit) to evaluate the quality of the system [16]. More precisely speaking, the quality of the system means that under certain bit error rate requirement, the highest transition bit rate and longest propagation length we can achieve. However, before we go to that part, we need to know what will distortion the optical signal – the optical pulse propagating in the fiber.

In general, two things will disturb the quality of optical signal and cause an error at the receiver side. First one is the power noise generated during the propagation period, which will be discussed in section 2.3; another is the pulse broadening due to the characteristic of the fiber [17], and the reason of the pulse broadening can be separated into two groups: linear effect and nonlinear effect. In section 2.1, the phenomena of linear effect will be introduced, and we will discuss how to deal with the broadening of the optical pulse. In section 2.2, the nonlinear effect is described. In section 2.3, we will see what should be considered when we want to estimate the quality of the optical communication system.

In the situation of low optical power and low bit rates in the optical system, we can assume that the refractive index is not affected by the optical power, and there is no

interaction between different optical signals, which means the fibers here are regarded as a linear medium. In this case, the signal will see some linear distortion effects. Such as modal dispersion: the spatial components in the multimode fiber propagated with different velocity; chromatic dispersion (CD): the spectral components (mainly in the single mode fiber) dispersed in time; and polarization mode dispersion (PMD) [18]: the two orthogonal polarization modes see different refractive indexes because of the birefringence effect due to asymmetric structure of the fiber.

However, high power lasers and new modulation techniques become more popular nowadays, which give us the ability to send more information at the same time. When we increase the optical power or the number of the channels in the fiber, the fiber here will become a nonlinear medium, and the signal will see some nonlinear distortion effects. Such us self-phase modulation (SPM): the pulse frequency instantaneously variate in time based on the Kerr effect; cross-phase modulation (XPM) [19]: the nonlinear phase shift of the signal in one channel is affected both by the power of that channel itself and the power of other channels; four-wave mixing (FWM): the mutual interaction between different optical signals generate a new signal with different frequency, and some nonlinear scattering (stimulated Raman scattering and stimulated Brillouin scattering).

In this thesis, we will focus on two effects: chromatic dispersion and self-phase modulation. For an optical transmission system with a single channel in single mode fiber, our goal is to increase the transmission bit rate for given signal power, SNR and propagation length. To approach higher transmission bit rate, we would like to shorten the pulse duration as much as possible. Thus, the pulse broadening and the pulse

attenuation in the fiber – due to chromatic dispersion and self-phase modulation, will be two major problems we have.

2.1 Chromatic dispersion

The reason why we have chromatic dispersion phenomena is that the group velocity is a function of wavelength in the fiber. Which means different wavelength parts of the same optical pulse propagate with different velocity, some wavelength parts will propagate faster than the other parts. Thus, after some propagation length, the pulse will broaden, and affect the optical pulse in another time slot. Here, group velocity is defined as $v_g = \left(\frac{d\beta(\omega)}{d\omega}\right)^{-1}$; where $\beta(\omega)$ is propagation constant, which can be expanded by Taylor's expansion (when optical pulse has narrow bandwidth of frequency ω, which is true in most of the cases in optical communication area) as [17]:

$$\beta(\omega) \cong \beta(\omega_0) + (\omega - \omega_0)\frac{d\beta}{d\omega}_{|\omega=\omega_0} + (\omega - \omega_0)^2 \frac{d^2\beta}{d\omega^2}_{|\omega=\omega_0} + (\omega - \omega_0)^3 \frac{d^3\beta}{d\omega^3}_{|\omega=\omega_0} \quad (1)$$

We can see that the first term in the denominator of group velocity $\frac{1}{v_g} = \left(\frac{d\beta(\omega)}{d\omega}\right)$ is constant $\left(\frac{d\beta}{d\omega}_{|\omega=\omega_0}\right)$. The second term is $2(\omega - \omega_0)\frac{d^2\beta}{d\omega^2}_{|\omega=\omega_0}$, which make the group velocity become frequency (wavelength) dependent if $\frac{d^2\beta}{d\omega^2}_{|\omega=\omega_0}$ is not zero. Due to this relation between $\frac{d^2\beta}{d\omega^2}_{|\omega=\omega_0}$ and group velocity v_g, this constant $\frac{d^2\beta}{d\omega^2}_{|\omega=\omega_0}$ is commonly known as group velocity dispersion (GVD) coefficient, $\beta_2 = \frac{d^2\beta}{d\omega^2}_{|\omega=\omega_0}$, often expressed

in $^{ps^2}/_{km}$. On the other hand, $\frac{d^3\beta}{d\omega^3}_{|\omega=\omega_0}$ is known as differential dispersion parameter β_3, often expressed in $^{ps^3}/_{km}$, which is related to the slop of chromatic dispersion.

In order to analyze the pulse broadening phenomena, we need to introduce some other parameters we use in the system. For the pulse propagate in the fiber, it is common to assume that the pulse shape is varying slowly, and we can use a Gaussian function to describe the pulse amplitude, $\mathrm{A}(0,\mathrm{t}) = A_0 \exp\left(-\frac{i\,C_0\,t^2}{2{\tau_0}^2}\right)\exp\left(-\frac{t^2}{2{\tau_0}^2}\right)$. Here, $A_0 = \sqrt{P_0}$ is the peak amplitude; P_0 is the peak power. The term $\exp\left(-\frac{t^2}{2{\tau_0}^2}\right)$ represent the Gaussian shape in the time domain. The term $\exp\left(-\frac{i\,C_0\,t^2}{2{\tau_0}^2}\right)$ represents the initial chirp (pre-chirp) of this pulse. It doesn't affect the envelope of the pulse, but it change the timing distribution of different wavelength group of the pulse. As mentioned above, some wavelength groups will propagate faster than others due to chromatic dispersion. This initial chirp can compensate a part of the dispersion and slightly suppress the broadening phenomena for short term transmission. The most important parameter here is τ_0, the half width at the $^1/_e$ maximum (HWEM) of power, which represent the pulse width. Fig. 1. Shows the amplitude and the power in the time domain, we can see that the power is about $e^{-1} \cong 0.36$ of the maximum at the time $\mathrm{t} = \tau_0$.

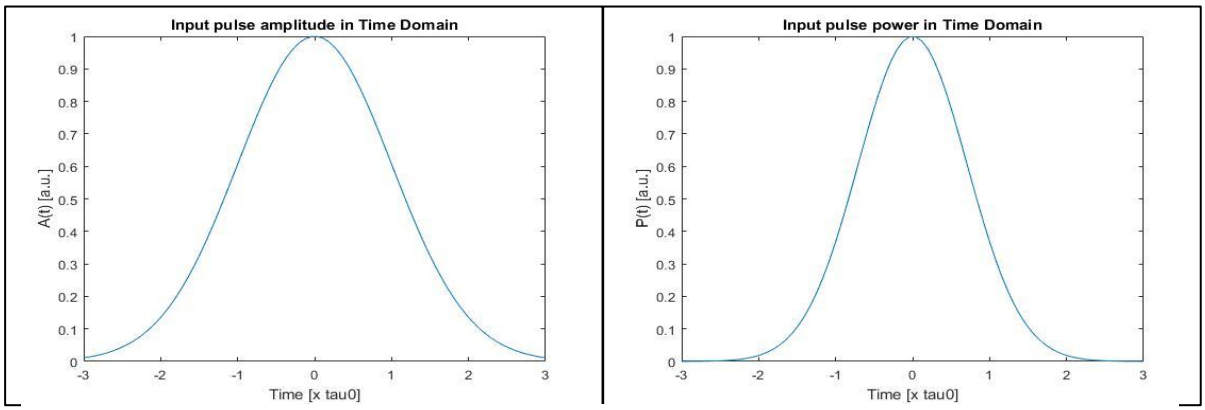

Fig. 1. Input pulse amplitude and power.

Now, we can take a look at the chromatic dispersion induced pulse broadening effect [20]:

$$\frac{\tau(z)}{\tau_0} = \sqrt{\left(1 + \frac{C_0 \beta_2 z}{{\tau_0}^2}\right)^2 + \left(\frac{\beta_2 z}{{\tau_0}^2}\right)^2 + \left(1 + {C_0}^2\right)\left(\frac{\beta_3 z}{2{\tau_0}^2}\right)^2} \qquad (2)$$

Here, τ_0 is the pulse width of input pulse, $\tau(z)$ is the pulse width at the propagation distance z.

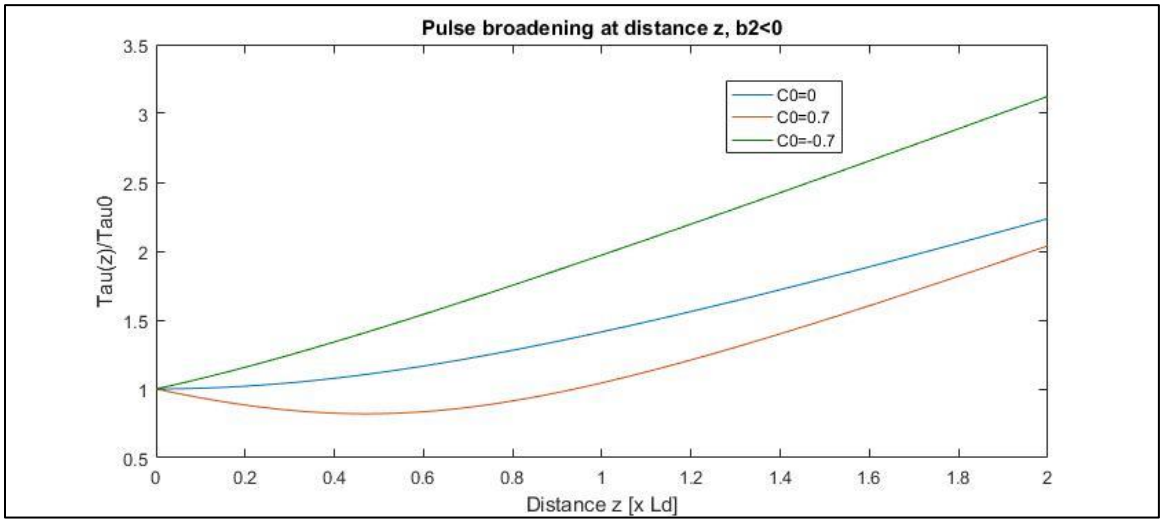

Fig. 2. Pulse broadening due to chromatic dispersion.

As seen in Fig. 2, the different pre-chirp coefficient can affect the development of pulse broadening development. If the pre-chirp coefficient has different sign with group velocity dispersion β_2, the term $\left(1 + \frac{C_0 \beta_2 z}{{\tau_0}^2}\right)^2$ can be less than one under certain distance z. However, it will not go to negative because the square and it will still growing with large z, so as other terms. On the other hand, since the pulse broadening comes from the delay between different wavelength groups, we can say that the broadened pulse also

become more chirped, and the chirp induced by the chromatic dispersion can be represented as:$C(\mathrm{z}) = C_0 + \left(1 + {C_0}^2\right)\frac{\beta_2 z}{{\tau_0}^2}$.

To reduce the impact of dispersion, we can have a different strategy for different transmission distance requirement. For a short transmission distance requirement (typically less than 40km), we can adjust the pre-chirp coefficient to maintain the pulse width under some tolerance. For higher transmission distance requirement, we need other technologies help.

In general, we have two ways to deal with dispersion. One is digital signal processing (DSP) method [21]. On the receiver side, after the optical signal is detected and translated to the electrical signal, we can use some DSP recover the broadened signal to the original shape. Another one is dispersion management method [22]. During the whole transmission distance requirement, we can insert some segments of dispersion compensating fiber (DCF) which has different sign of chromatic dispersion β_2 with the single mode fiber (SMF) we used for propagation. In this thesis, we will focus on dispersion management method and discuss more about that.

For dispersion compensation, we have to calculate the length of the DCF we need for the system. We can review the meaning of the dispersion again and see the pulse broadening from another perspective. In the very beginning, dispersion phenomena comes from the difference of the group velocity between different wavelength, $v_g = \left(\frac{d\beta(\omega)}{d\omega}\right)^{-1}$. We can say that the propagation time for a distance L of a particular group is $\tau_g = \frac{L}{v_g} = L\left(\frac{d\beta(\omega)}{d\omega}\right)$. Thus, the pulse broadening effect can be described by the difference of the arriving time between different group, $\Delta\tau_g = \frac{d\tau_g}{d\omega}\Delta\omega = L\left(\frac{d^2\beta(\omega)}{d\omega^2}\right)\Delta\omega$. For an optical pulse at

particular wavelength with spectral width $\Delta\omega$, the pulse broadening become $\Delta\tau_g = L\,\beta_2\,\Delta\omega$. Here, we can see that the order of propagation length L and GVD coefficient β_2 is the same. In other words, in order to compensate the pulse broadening cause by the chromatic dispersion, the length of DCF and SMF need to satisfy $L_{SMF}\,\beta_{2,SMF} + L_{DCF}\,\beta_{2,DCF} = 0$. For example, if we use 80km long SMF, and the GVD coefficient of SMF and DCF are $\beta_{2,SMF} = -20\ {}^{ps^2}/_{km}$ and $\beta_{2,DCF} = 127.5\ {}^{ps^2}/_{km}$, we will need about 12.55 km of DCF to compensate the chromatic dispersion.

There are three types of the dispersion compensation map. First one is pre-compensation: put all the DCF we need in front of the SMF; the second one is post-compensation: put all the DCF after the SMF; the third one is the combination of the first and second types: put half DCF in the front and a half in the end.

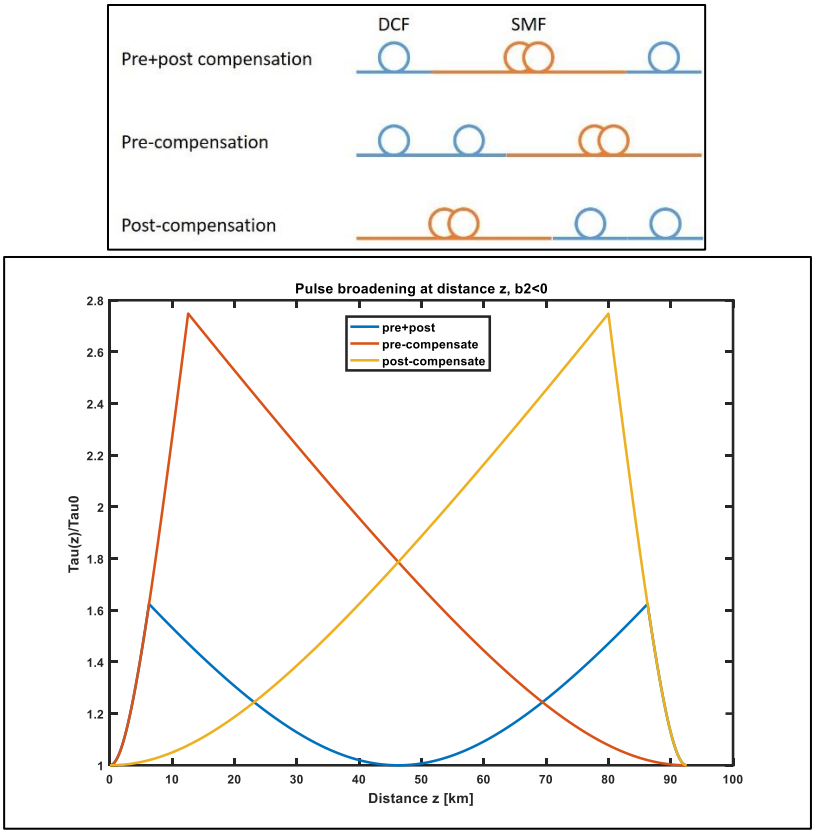

Fig. 3. Dispersion management map and pulse broadening.

From Fig. 3, it is obvious that in the case of pre- and post-compensation, the pulse width will become very broad during the propagation. If we only consider the dispersion, they are the same, all of them can compensate the dispersion and recover the pulse shape. However, the pulse will also see the nonlinear effect in the fiber. As mentioned at the beginning of this Chapter, four-wave mixing is a nonlinear effect that will generate a new frequency of light due to the interaction of two different frequency components. If the pulse width becomes too broad to interact with another pulse, the quality of the signal decreases because of this nonlinear effect.

To sum up, we will use pre- plus post-compensation strategy to deal with the dispersion, so we can maintain the pulse width to be always less than two times of the original value.

2.2 Nonlinear Kerr effect

In the last section, we have known the reason why chromatic dispersion will cause pulse broadening and how we deal with it. Now, we will discuss why nonlinear Kerr effect will also affect the pulse width.

The phenomena of pulse width changing due to nonlinear Kerr effect starts from the property of the reflection index of the fiber. When the optical power is low in the fiber, the reflection index is almost constant and will not change with the power. However, when the optical power is high enough, the reflection index become power dependent. Due to the time-varying property of the pulse power, we can see that the reflection index become a function of time. Further, it will cause a time-varying phase shift on the pulse, called self-phase modulation (SPM). Since the frequency is the changing rate of the phase, SPM will make the pulse more chirped. In the end, this more chirped pulse will broaden (or shorten, depends on the initial chirp) during the propagation because of the chromatic dispersion.

Now, we can rewrite the pulse broadening effect and take the nonlinear Kerr effect into account this time. For the evaluation of an un-chirped Gaussian pulse propagation in the fiber, including the impact of chromatic dispersion and self-phase modulation, the pulse broadening effect can be represented as [20]:

$$\frac{\tau(z)}{\tau_0} = \sqrt{1 + \frac{\sqrt{2}L_{eff}}{L_{nel}}\frac{\beta_2 z}{{\tau_0}^2} + \left(1 + \frac{4}{3\sqrt{3}}\frac{{L_{eff}}^2}{{L_{nel}}^2}\right)\left(\frac{\beta_2 z}{{\tau_0}^2}\right)^2} \quad (3)$$

Here, the effective length $L_{eff} = \frac{1-\exp(-\alpha L)}{\alpha}$ comes from the considering of the fiber loss α. Since the nonlinear effect depends on the pulse power, and the power will continuous decay during the propagation because of the fiber loss, the meaning of the effective length is that the pulse will use the same power acting with the fiber and see the same nonlinear effect as the situation that the power decrease with the whole length L. L_{nel} is nonlinear length that means the maximum nonlinear phase shift at this effective length is 1 rad, $L_{nel} = \frac{1}{\gamma P_0}$. γ is the nonlinear coefficient of the fiber and P_0 is the input peak power. There are three terms in this representation, first term 1 and third term $\left(1 + \frac{4}{3\sqrt{3}}\frac{{L_{eff}}^2}{{L_{nel}}^2}\right)\left(\frac{\beta_2 z}{{\tau_0}^2}\right)^2$ are always positive and third grows very fast. The second term $\frac{\sqrt{2}L_{eff}}{L_{nel}}\frac{\beta_2 z}{{\tau_0}^2}$ can be negative and slow down the growing rate of pulse width if the GVD coefficient is negative, which is the case of SMF. That is because the chirp induced by the nonlinear Kerr effect always has the same direction. In the leading edge, the pulse power is increasing, the reflection index is increasing nonlinearly, $\mathrm{n(P)} = n_0 + n_2\frac{P}{A_{eff}}$, the nonlinear phase shift is decreasing (like a modulation on the phase), and the frequency variation (which is derivative of the phase shift) is negative. It is known as red-shift (frequency decrease and wavelength increase). In the trailing edge, the pulse power is decreasing nonlinearly, cause a positive frequency variation, which is known as blue-shift. Thus, this self-phase modulation effect can also be seen as chirping because it change the timing distribution of different wavelength groups. Further, if this chirped pulse

propagate in a fiber whose chromatic dispersion chirp the pulse in the inverse way, they may compensate a part of each other and slow down the growing rate of pulse width.

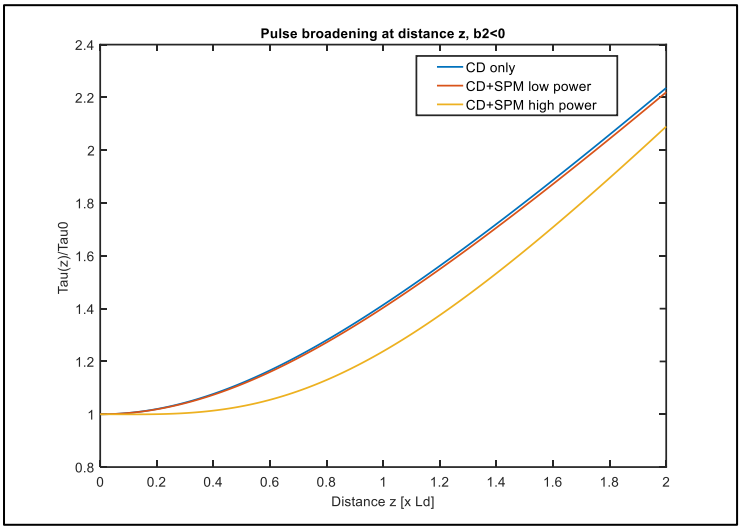

Fig. 4.pulse broadening induced by dispersion and SPM.

Fig. 4 represents the pulse broadening effect including the chromatic dispersion and self-phase modulation. In the low power case, the nonlinear effect is small; the pulse is broadened just like the case without nonlinearity. In the high power case, a part of the chromatic dispersion and self-phase modulation compensate each other and slow down the broadening effect. Now, we may ask what power is high enough to see the compensation.

It is common to use a parameter [20], $N^2 = \frac{L_D}{L_{nel}}$, to describe the strength of chromatic dispersion and self-phase modulation. L_D is called dispersion length, which means an unchirped Gaussian pulse will have broadening ratio of $\sqrt{2}$ when it propagate to this length without nonlinear effect. When this parameter N is much smaller than 1, it is dispersion dominate, the broadening of the pulse is primary due to the chromatic

dispersion, like the low power case in the figure. If this parameter N is close to 1, the dispersion and SPM are similar, the pulse width will grow very slowly, like the beginning of the high power case in the figure above. In the case of the parameter much higher than 1, the broadening effect is dominated by SPM. The reason why we don't show this case in the figure is that the mathematical representation of broadening effect in this section is just an approximation. To know the accurate broadening effect considering dispersion and SPM, we need to solve the nonlinear Schrodinger equation (NLSE), which will be described in Chapter 3.

2.3 Fiber Loss, OSNR, and BER

After the discussion of the chromatic dispersion and nonlinear Kerr effect of the fiber, here comes the last important property of the fiber – the fiber loss. Unlike the dispersion and SPM, the fiber loss doesn't affect the pulse shape; it decreases the pulse power. Before the optical amplifier is developed, we receive the signal and regenerate the signal to increase the transmission length; after we have the optical amplifier in the market, we can simply amplifier the pulse power to maintain the power and extent the transmission length. However, it also brings some side effects, and the most obvious problem is the spontaneous emission of the gain media in the amplifier. The spontaneous emission will propagate with the signal and be amplified by the next optical amplifier, called the amplified spontaneous emission (ASE) noise. The receiver will detect both of ASE noise and the signal; the ASE noise will affect the calculated signal power and cause an error.

Further, since the output power of the amplifier is the summation of ASE noise and the signal power, the more ASE noise generated by the amplifier, the less signal power can be propagated. The ratio between optical signal and noise power (OSNR) will become lower and lower, and error rate of the system will become higher and higher, like Fig. 5. In the following, we will introduce how to calculate the ASE noise power and the relation between ASE noise power and the error rate of the system.

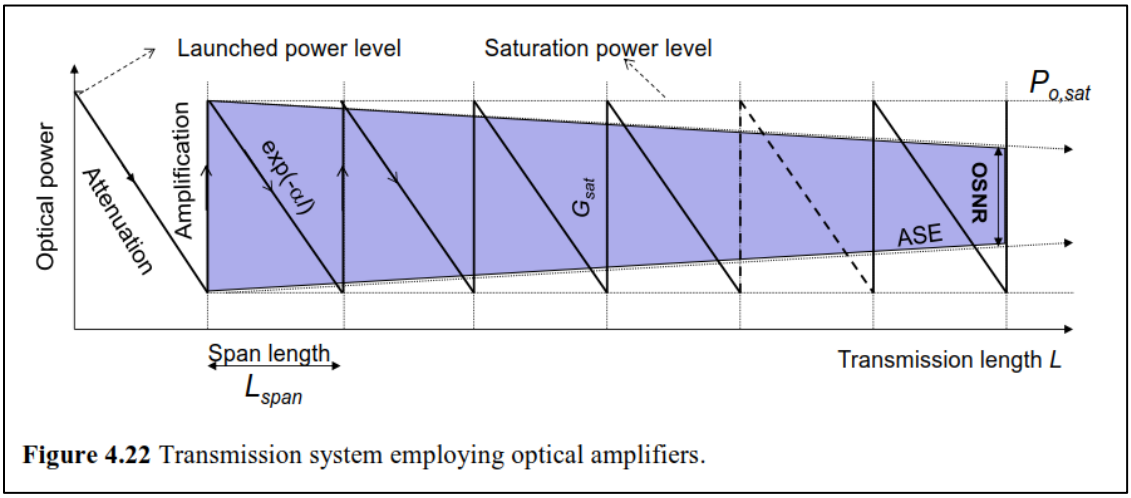

Figure 4.22 Transmission system employing optical amplifiers.

Fig. 5 OSNR behavior versus transmission length [17]

In theory [17], the spontaneous emission power can be represented as:

$$P_{sp}(\nu) = (G-1)\, NF_{no}\, h\nu\, B_{op} \qquad (4)$$

where G is the gain of amplifier, $G = \frac{P_{out}}{P_{in}}$. If there are no amplification, $G = 1$, there are no spontaneous emission noise. NF_{no} is the noise figure of the optical amplifier, which is the optical signal to noise ratio relation between the input and output, $NF_{no} = \frac{OSNR_{in}}{OSNR_{out}}$. $h\nu$ is the power of the photon. B_{op} is the bandwidth of the optical amplifier. From the relation we can see that for the noise power point of view, we should use more amplifier

and chose the gain value as low as possible to minimize the noise power. For example, if we need to amplifier the signal 100 times, in the case of one amplifier, the gain $G = 100$. In the case of two amplifier, each one will have gain $G = 10$. Thus, the total ASE noise power will be $P_{sp,one\ AMP}(\nu) = 99\ NF_{no}\ h\nu\ B_{op}$ and $P_{sp,two\ AMP}(\nu) = 2 * 9\ NF_{no}\ h\nu\ B_{op}$. The case using two amplifier has ASE noise power less than the case using one amplifier. However, we also need to consider the cost since the optical amplifier is expensive. It becomes a trade-off between price and noise power.

In general, for a system using SMF as the propagation media, we put optical amplifier tens of kilometers a time to compensate the loss of the fiber, and the gain we chose is just enough to compensate the loss of that segment of fiber. Thus, the total ASE noise power will be

$$P_{sp,total}(\nu) = N\ (G - 1)\ NF_{no}\ h\nu\ B_{op} \quad (5)$$

N is the number of the amplifier we use, $N = \frac{L}{L_{span}}$. L is the total propagation length, and L_{span} is the distance between two optical amplifier. Moreover, the OSNR at the receiver side can be represented as

$$OSNR = \frac{P_{sig}}{P_{noise}} = \frac{P_{ch} - P_{sp,total}(\nu)}{P_{sp,total}(\nu)} \quad (6)$$

P_{ch} is the channel power, the averaged power of particular wavelength.

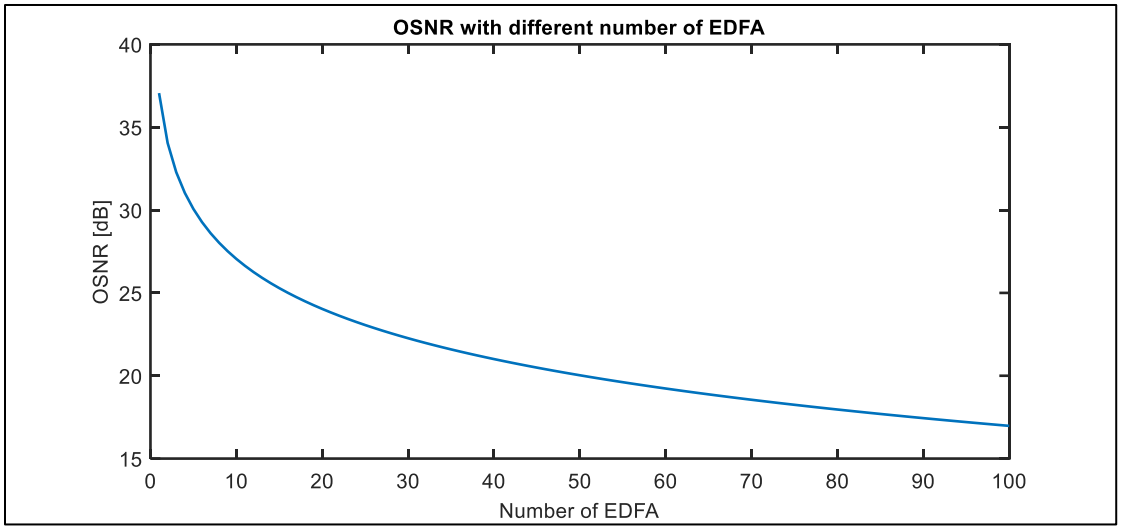

Fig. 6. OSNR development versus the number of the EDFA

Fig. 6 is an example of the OSNR performance versus the number of EDFA we use. The gain of EDFA is chosen to compensate the loss of 80km SMF, $G = 0.2 \times 80\ \text{dB} \cong 40$. The noise figure of EDFA is typical $5\ \text{dB}$. Optical bandwidth is typical $12.5\ \text{GHz}$. We can see that the OSNR decrease very fast in the beginning. If we want to have OSNR higher than 20 dB, we need to control the number of EDFA lower than 50.

From the discussion above, we can see that the longer distance we want to achieve, the more amplifier we need to use, the larger ASE noise it will generate, and the lower OSNR we will get on the receiver. But what is the lowest OSNR we can accept, it will depend on the relation between OSNR and bit error rate (BER), and this relation will be different when we use different kinds of signal.

We start from the simplest signal, the return to zero (RZ) coding, 2-level pulse amplitude modulated signal (2-PAM). This kind of signal always has the same pulse width, since it will return to zero in each time slot, and it only has two possible pulse amplitude 1 and 0, or 1 and -1, depends on the detection technique. For direct detection scheme, we can only

detect the power of the signal; the amplitude is 1 or 0, the BER of this 2-PAM signal can be represented as

$$BER_{2PAM,DD} = P_{e,2PAM,DD} = \Psi\left(\sqrt{\frac{E_b}{N_0}}\right) = \frac{1}{2}\mathrm{erfc}\left(\sqrt{\frac{E_b}{2N_0}}\right) \quad (7)$$

Erfc (x) is the complementary error function, $erfc(\mathrm{x}) = \frac{2}{\sqrt{\pi}}\int_x^{\infty} e^{-y^2}dy$. $\frac{E_b}{N_0}$ is the information signal to noise ratio which has relation with OSNR above, $\frac{E_b}{N_0} = \frac{2\,B_{op}}{R_{s,info}}\frac{OSNR}{log_2 L}$. $R_{s,info}$ is the information symbol rate, and M means the modulation level. On the other hand, if we use coherent detection, we can measure the phase of the optical signal, amplitude of the 2-PAM signal can be 1 and -1, the power is the same, but has phase shift of π. The BER of the 2-PAM using coherent detection can be

$$BER_{2PAM,CD} = P_{e,2PAM,CD} = \Psi\left(\sqrt{\frac{2E_b}{N_0}}\right) = \frac{1}{2}\mathrm{erfc}\left(\sqrt{\frac{E_b}{N_0}}\right) \quad (8)$$

For example, there is a 2-PAM signal whose $\mathrm{OSNR} = 10$, information symbol rate $R_{s,info} = 10\ {GS}/{s} = 10\ {Gb}/{s}$, optical bandwidth of EDFA is typical 0.1nm, $B_{op} = 0.1\ nm = 12.5\ GHz$. Then $BER_{2PAM,DD} \cong 2.9 \times 10^{-7}$, $BER_{2PAM,CD} \cong 7.7 \times 10^{-13}$. The following figure is the BER performance of 2-PAM signal, it's obvious that the coherent detection case move to error free region faster than direct detection case. (in practice, 10^{-12} of BER is low enough to be regard as error free region) Fig. 7 is the BER behavior of a 2-PAM signal with direct detection and coherent detection. Within the same BER requirement, system using direct detection always need to have about 3dB information SNR higher than the system using coherent detection.

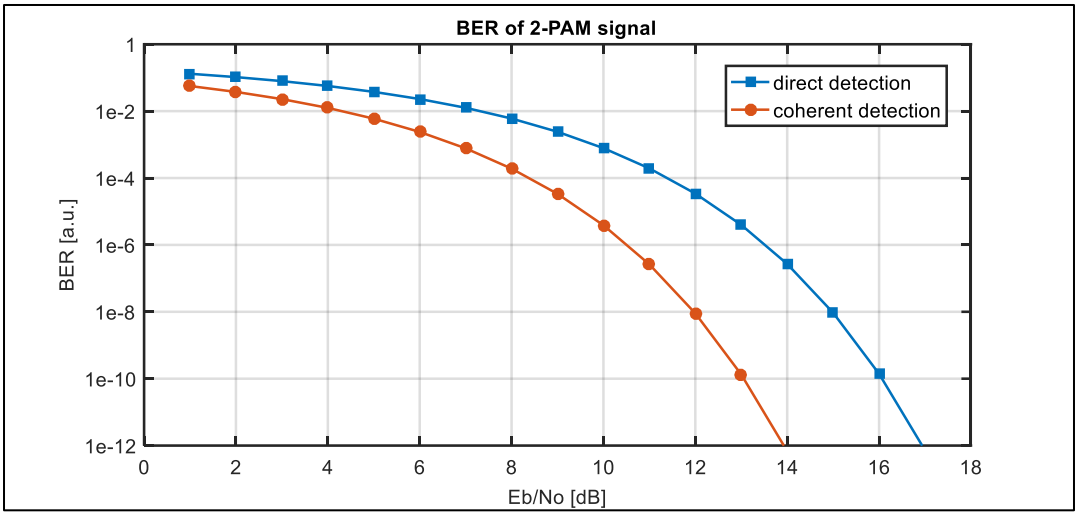

Fig. 7. BER development versus the information SNR of a 2-PAM signal.

In more general case, for an L-PAM signal using coherent detection, the BER can be

$$BER_{L-PAM,CD} \cong \frac{P_{e,L-PAM,CD}}{log_2 L} = \frac{1}{log_2 L}\frac{L-1}{L}\operatorname{erfc}\left(\sqrt{\frac{3}{L^2-1}\frac{E_b\, log_2 L}{N_0}}\right) \quad (9)$$

$P_{e,L-PAM,CD}$ is the symbol error rate. Since one L-PAM pulse has L kinds of different amplitude, one L-PAM symbol represent $log_2 L$ bits. For example, 4-PAM can represent two bits, and four amplitude represent 00, 01, 10, and 11.

Now, we can take a look at more complicated modulation format. Thanks for the coherent detection technique, we can extract the phase information of the received signal. Quadrature amplitude modulation (QAM) is a modulation format that loads the information on the pulse amplitude and phase. We can regard QAM signal as the span of two basis signal, each has PAM format, and there is phase shift of $\frac{\pi}{2}$ between them. Fig. 8 is the constellation diagram of the QAM signal with different modulation level (with same symbol power).

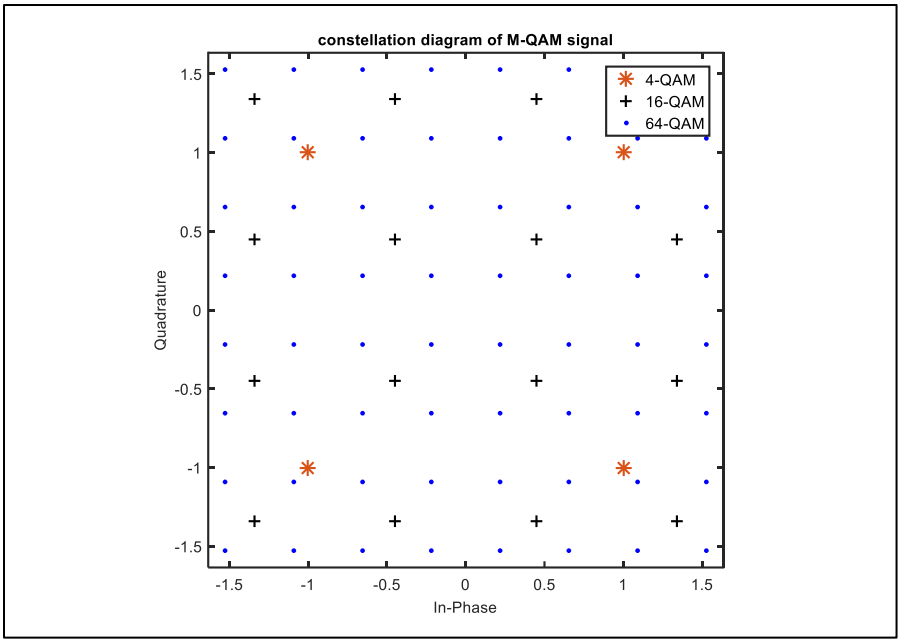

Fig. 8. Constellation diagram of 4-QAM, 16QAM, and 64-QAM signal.

Thus, the BER of an M-ary QAM signal (2D span of two L-PAM signals, L = $\sqrt{M}$) can be represented as

$$BER_{M-QAM} \cong \frac{P_{e,M-QAM}}{log_2 M} = \frac{1-\left(1-P_{e,L-PAM,CD}\right)^2}{log_2 M} = \frac{1}{log_2 M}\left\{1-\left[1-\frac{\sqrt{M}-1}{\sqrt{M}}\ erfc\left(\sqrt{\frac{3}{2(M-1)}\frac{E_{s,QAM}}{N_0}}\right)\right]^2\right\} \quad (10)$$

In the right-hand side, $\frac{E_{s,QAM}}{N_0}$ is the information symbol SNR of the QAM signal, which has relation with OSNR, $\frac{E_{s,QAM}}{N_0} = \frac{2\,B_{op}}{R_{s,info}} OSNR,\ E_{s,QAM} = 2\,E_{s,PAM} = 2\,E_{b,PAM}\ log_2 L.$

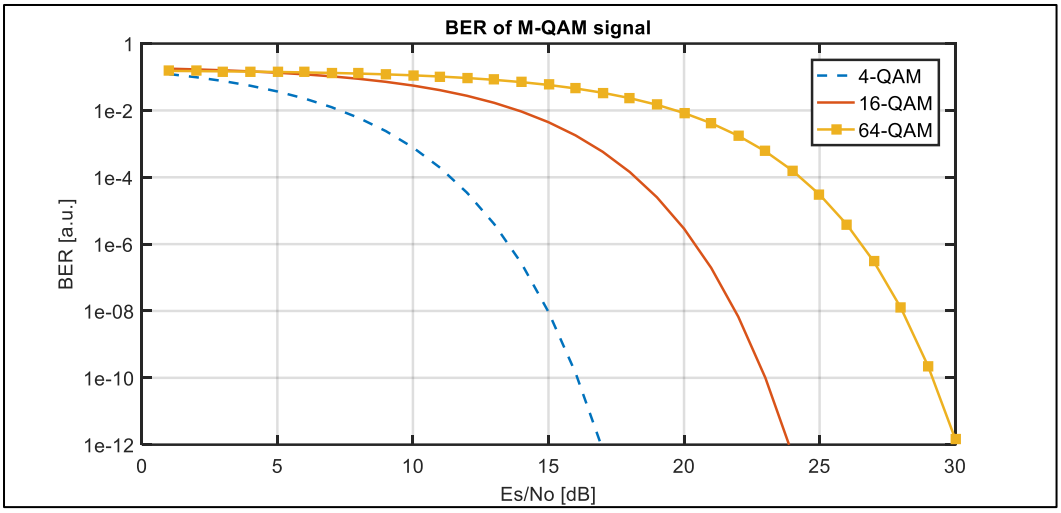

Fig. 9. BER behavior versus information SNR of 4-QAM, 16-QAM, and 64-QAM signal.

Fig. 9 shows the BER performance of the QAM signal with different modulation level. Under same electrical signal symbol to noise ratio, the higher modulation level has higher BER. Since the distance between constellation points become smaller when the modulation level increase, the higher modulation level signal is more sensitive to the noise.

In Chapter 3, we will combine all the discussion in this Chapter and use MATLAB to simulate the performance of an optical communication system.

Chapter 3

Numerical method and result

3.1 Modeling of signal propagation and detection

In Chapter 2 we have introduced that three main problems will affect the quality of the signal, and how we evaluate the performance of an optical communication system. However, the mathematical representation in Chapter 2 is only an approximation. For a more precise description, we need to use a more accurate model, which is nonlinear Schrodinger equation. In the following section, we will introduce this equation, how to solve the equation, and how to use the result to evaluate the performance of the optical communication system.

3.1.1 Nonlinear Schrodinger equation

Including the impact of the fiber attenuation, chromatic dispersion, and nonlinear Kerr effect, the generalized nonlinear Schrodinger equation has the form [17]:

$$\frac{\partial \mathrm{A(z,t)}}{\partial \mathrm{z}} + \beta_1 \frac{\partial \mathrm{A(z,t)}}{\partial \mathrm{t}} + \frac{i\beta_2}{2}\frac{\partial^2 \mathrm{A(z,t)}}{\partial \mathrm{t}^2} - \frac{\beta_3}{6}\frac{\partial^3 \mathrm{A(z,t)}}{\partial \mathrm{t}^3} = i\gamma|\mathrm{A(z,t)}|^2\mathrm{A(z,t)} - \frac{1}{2}\alpha\mathrm{A(z,t)} \quad (11)$$

As mentioned, β_3 is much smaller than the β_2, and the β_1 term only represents the time delay between input and output so that we can ignore these two terms and the consolidated equation becomes:

$$\frac{\partial \mathrm{A(z,t)}}{\partial \mathrm{z}} = i\gamma|\mathrm{A(z,t)}|^2\mathrm{A(z,t)} - \frac{1}{2}\alpha\mathrm{A(z,t)} - \frac{i\beta_2}{2}\frac{\partial^2 \mathrm{A(z,t)}}{\partial \mathrm{t}^2} \quad (12)$$

Here, $\mathrm{A(z,t)}$ is the pulse shape function we want to know, and the input pulse we use is pre-chirped Gaussian pulse $\mathrm{A(0,t)} = A_0 \exp\left(-\frac{i\,C_0\,t^2}{2{\tau_0}^2}\right)\exp\left(-\frac{t^2}{2{\tau_0}^2}\right)$, as we mentioned in section 2.1. On the right hand side, there are three terms. First term $i\gamma|\mathrm{A(z,t)}|^2\mathrm{A(z,t)}$ represent the nonlinear effect (self-phase modulation mentioned in section 2.2). Second term $-\frac{1}{2}\alpha\mathrm{A(z,t)}$ is associated to fiber loss. Third tem $-\frac{i\beta_2}{2}\frac{\partial^2 \mathrm{A(z,t)}}{\partial \mathrm{t}^2}$ describe the chromatic dispersion. On the left side, $\frac{\partial \mathrm{A(z,t)}}{\partial \mathrm{z}}$ is the development of the pulse shape. If we know the representation of right hand side mathematically, we can calculate the shape function at z1 $\mathrm{A(z1,t)}$ by the function at z0 $\mathrm{A(z0,t)}$.

There are two well-known methods to solve the equation: Finite-difference method [23] and split-step Fourier method [24]. The former one uses some schemes to approximate the time differential terms in the equation; the latter one uses the Fourier transform to solve the problem in the frequency domain. It is said that for a system whose carrier pulse has a slowly varying amplitude, the split-step Fourier method is the more efficient way to solve the equation. Therefore, in this thesis, we will use split-step Fourier method (SSFM) to solve the nonlinear Schrodinger equation.

3.1.2 Split-step Fourier method

The main point of this method is to split the whole transmission length into many small segments, and assume that the segment is small enough that the linear and nonlinear part of this segment can act independently. Thus, we can split the solving process into two steps. The first step we deal with the linear part and assume there is no nonlinear effect. The second step we deal with the nonlinear part and assume there is no linear effect.

Mathematically, it is done by rewriting the nonlinear Schrodinger equation into this form: $\frac{\partial \mathrm{A(z,t)}}{\partial \mathrm{z}} = \left(\widehat{\mathrm{D}} + \widehat{\mathrm{N}}\right) \mathrm{A(z,t)}$, while $\widehat{\mathrm{D}}$ is the linear operator, $\widehat{\mathrm{D}} = -\frac{\mathrm{i}\beta_2}{2}\frac{\partial^2}{\partial \mathrm{t}^2} - \frac{\alpha}{2}$; $\widehat{\mathrm{N}}$ is the nonlinear operator, $\widehat{\mathrm{N}} = \mathrm{i}\gamma|\mathrm{A(z,t)}|^2$. After that, since the step size $\Delta \mathrm{z}$ is small, it can be approached by

$$\mathrm{A(z + \Delta z, t)} \cong \exp\left(\widehat{\mathrm{N}}\,\Delta \mathrm{z}\right) \exp\left(\widehat{\mathrm{D}}\,\Delta \mathrm{z}\right) \mathrm{A(z,t)} \qquad (13)$$

For the linear part, we can evaluate the operator in the Fourier domain:

$$\exp\left(\widehat{\mathrm{D}}\,\Delta \mathrm{z}\right) \mathrm{A(z,t)} = FT^{-1}\left\{\exp\left[\left(\frac{\mathrm{i}\beta_2}{2}\omega^2 - \frac{\alpha}{2}\right)\Delta \mathrm{z}\right] FT\{\mathrm{A(z,t)}\}\right\} \qquad (14)$$

For the nonlinear part, it can be approached by

$$\exp\left(\widehat{\mathrm{N}}\,\Delta \mathrm{z}\right) \mathrm{A(z,t)} = \exp(i\gamma|A(z,t)|^2 \Delta \mathrm{z})\, \mathrm{A(z,t)} \qquad (15)$$

Further, there is a more accurate way to calculate the $\mathrm{A(z + \Delta z, t)}$, which is symmetric split-step Fourier method (S-SSFM), just separate the linear step into two pieces:

$$A(z+\Delta z,t) \cong \exp\left(\widehat{D}\frac{\Delta z}{2}\right)\exp(\widehat{N}\Delta z)\exp\left(\widehat{D}\frac{\Delta z}{2}\right)A(z,t) \quad (16)$$

At this time, we calculate the linear operator with half step size first, $A\left(z+\frac{\Delta z}{2},t\right) \cong \exp\left(\widehat{D}\frac{\Delta z}{2}\right)A(z,t)$. And then operate the nonlinear part at the middle point:

$$\exp(\widehat{N}\,\Delta z)\,A\left(z+\frac{\Delta z}{2},t\right) = \exp\left(\int_z^{z+\Delta z}\widehat{N}(z')\Delta z'\right)A\left(z+\frac{\Delta z}{2},t\right)$$

$$\cong \exp\left(\frac{\widehat{N}(z)+\widehat{N}(z+\Delta z)}{2}\Delta z\right)A\left(z+\frac{\Delta z}{2},t\right) \cong \exp\left[\widehat{N}\left(z+\frac{\Delta z}{2}\right)\Delta z\right]A\left(z+\frac{\Delta z}{2},t\right) \quad (17)$$

Finally, we operate the linear part with the rest half step size to get $A(z+\Delta z,t)$.

Here, I use this algorithm to solve the nonlinear Schrodinger equation in the MATLAB. Fig. 10 shows the simulation result of the simplest case.

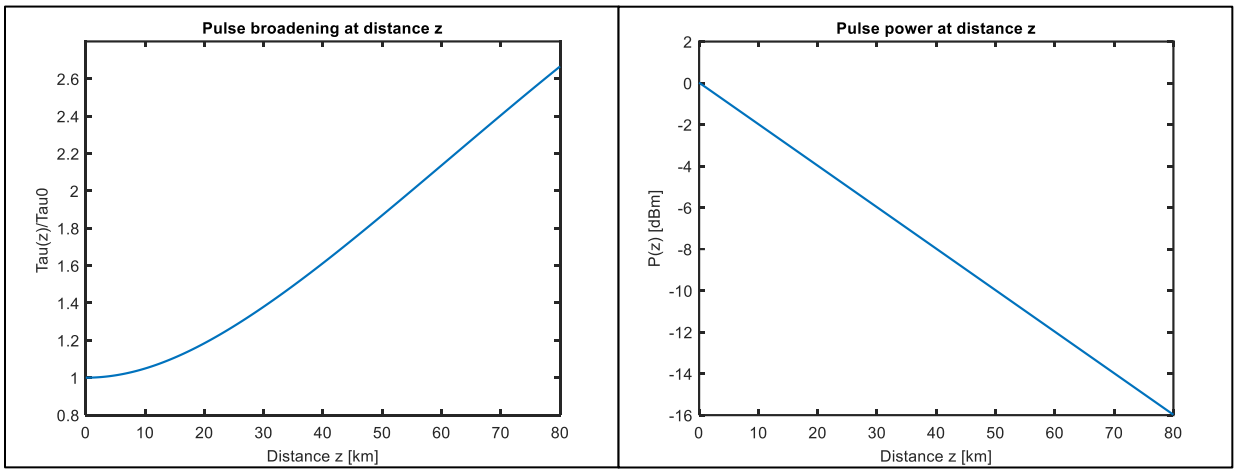

Fig. 10. Pulse broadening and power decay simulated by SSFM.

Fig. 10 is the pulse broadening behavior and averaged power behavior of an unchirped Gaussian pulse propagating in the SMF. The parameters of the fiber here are: GVD coefficient $\beta_2 = -20\ {}^{ps^2}/_{km}$; transmission length $L = 80\ km$; nonlinearity coefficient $\gamma = 1.3\ {}^{1}/_{W\ km}$. The parameter of the pulse are: symbol rate $R_s = 10\ {}^{GS}/_{s}$;

corresponding time slot $T_s = \frac{1}{R_s} = 100\ ps$; initial pulse width $\tau_0 = \frac{T_s}{4} = 25\ ps$, which is chosen to be $1/4$ of time slot in order to have most of the power inside the time slot; averaged pulse power $P_{avg} = 0\ dBm = 1\ mW$, which is common used in the industry; corresponding peak power and peak amplitude can be calculated by the relation $\frac{\int_{-\frac{T_s}{2}}^{\frac{T_s}{2}} |A(z,t)|^2 dt}{T_s} = P_{avg}$, in this case will be $P_0 \cong 2.27\ mW$ and $A_0 = \sqrt{P_0} \cong 1.51\ \sqrt{mW}$.

As mentioned in Chapter 2, we can calculate the dispersion length and nonlinear length from the parameters above to see if this signal is dispersion dominated or nonlinear dominated. $L_D = \frac{{\tau_0}^2}{|\beta_2|} = 31.25\ km$, $L_{NL} = \frac{1}{\gamma P_0} \cong 339\ km$, the parameter $N^2 = \frac{L_D}{L_{nel}} \cong 0.092$, N $\cong 0.304$, it's smaller than one, but not too much, so we can imagine that the chromatic dispersion are stronger than self-phase modulation in this case.

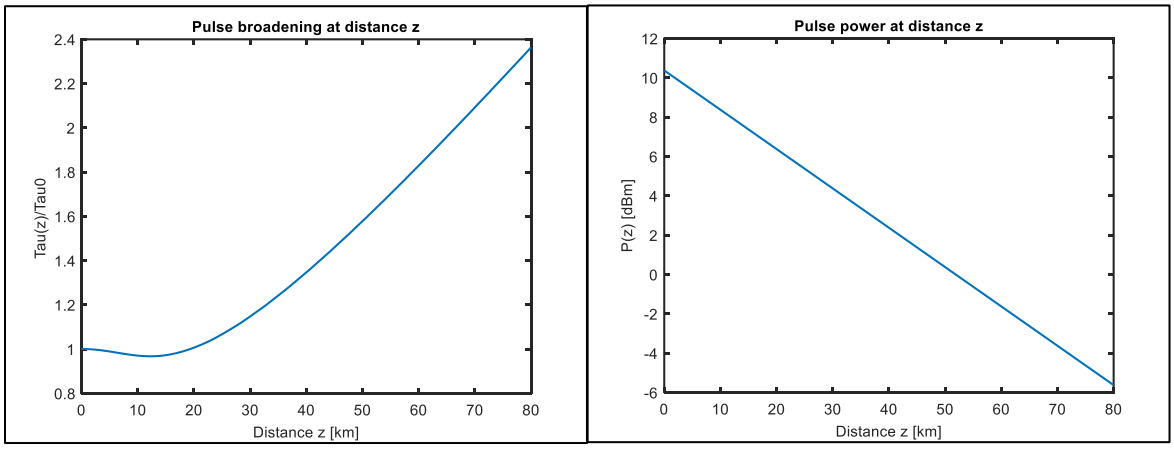

Fig. 11. Pulse broadening and power decay of high input power.

Fig. 11 is the high power case. The averaged power is about 10.35 dBm, which make $L_D = L_{NL} = 31.25\ km$. Compare to the 0 dBm case, the pulse width in this case maintain nearly the same in the beginning 20km. After that, the pulse start broaden because the nonlinearity decrease due to the decaying power. Thus, if we turn off the fiber loss, like

Fig. 12, we can see that the dispersion and self-phase modulation compensate many of each other and the pulse width grow very slow.

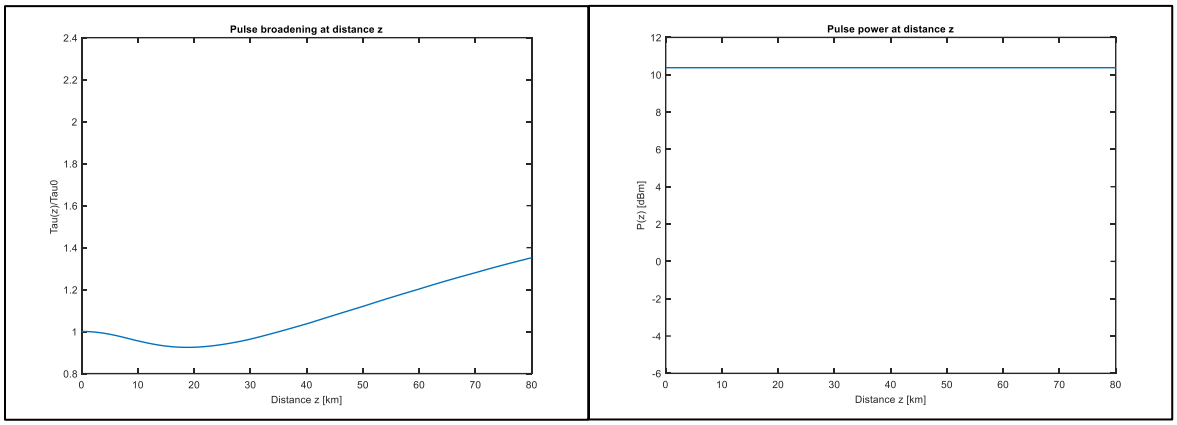

Fig. 12. Pulse broadening and power decay of high input power without fiber loss.

Now, as we mentioned in Chapter 2, we can use DCF to compensate the dispersion and use amplifiers to compensate the fiber loss. Fig. 13 is the structure.

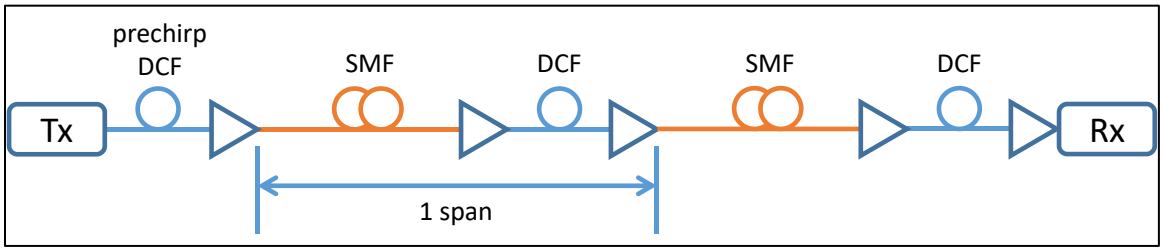

Fig. 13. Structure of the communication system.

As the figure in section 2.1, the first segment of DCF in front of the transmitter is used as pre-compensation fiber. Here, it can be regarded as pre-chirp DCF. The following segment of SMF, $L_{SMF} = 80\ km$, segment of DCF, $L_{DCF} = 12.55\ km$, and two amplifier constitute a single span. The total loss of one span is $80\ km \times 0.2\ {}^{dB}/_{km} + 12.55\ km \times 0.5\ {}^{dB}/_{km} = 22.275\ dB$. The gain of this two amplifier is chosen to be similar in order to minimize the ASE noise power, here is 11.1 dB and 11.175 dB.

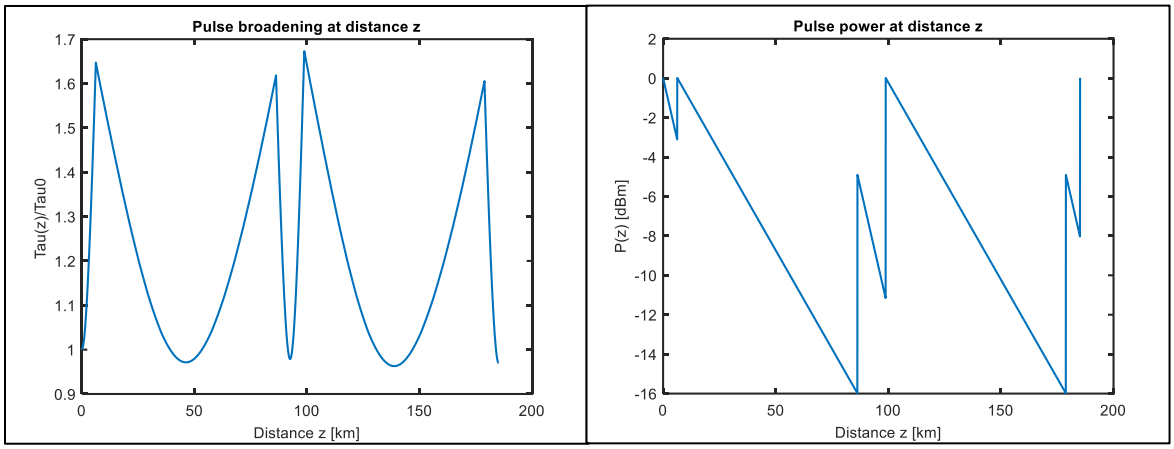

Fig. 14. Pulse broadening and power behavior of 2 span propagation.

Fig. 14 is the pulse broadening and power behavior of the structure above. The slowly changing curve stands for the propagation in SMF, the fast changing curve represent the propagation in DCF. The length of the DCF in the second (final) span is half because the other half is placed in front of the transmitter. After these two span propagation, the pulse width is recovered to the original value, and the power is also recovered to the initial.

3.1.3 Bit error rate calculation

In the section 3.1.2, we use S-SSFM to solve the nonlinear Schrodinger equation in the MATLAB and evaluate the pulse width and power behavior in the communication system. Now, we will introduce how to add the ASE noise on the signal and calculate the BER in the MATLAB.

In general, we usually use awgn() function (add white Gaussian noise to signal), to add the noise to the signal or use wgn() function (generate white Gaussian noise) to create the noise. There are two bullied in function in the MATLAB we use to generate the noise

with Gaussian distribution property. In the awgn() function, we need to know the signal to noise ratio of the information (SNR) to complete the process. The algorithm is like this: we have a series of pulse amplitude, $\{A_1, A_2, \dots, A_N\}$, if there are no initial noise, all the amplitude will be the same; then we use the ASE noise power to calculate the SNR in the awgn() function; finally, put the information into the awgn() function, it will give me a new series of pulse amplitude with noise $\{A'_1, A'_2, \dots, A'_N\}$. The distribution of this series is Gaussian distribution, and the variance will be the noise power. In the wgn() function, we can use ASE noise power to generate a series of noise amplitude $\{N_1, N_2, \dots, N_N\}$, whose variance is the noise power; and add this noise amplitude on the signal pulse amplitude, $\{A'_1, A'_2, \dots, A'_N\} = \{A_1 + N_1, A_2 + N_2, \dots, A_N + N_N\}$. For example, in the case of 2-PAM signal using coherent detection, the averaged pule power is 0 dBm, and peak power is 2.267 mW. If we have an averaged ASE noise power $P_{ASE} = -3$ dBm $\cong$ 0.5 mW , then the OSNR $= 3$ dB and corresponding information SNR $= \frac{E_S}{N_0} = \frac{2\,B_{op}}{R_{s,info}} OSNR \cong 4.99 \cong 6.98$ dB. The pule amplitude distribution is shown in here. Signal peak amplitude $A_0 = \sqrt{P_0} \cong 1.506\,\sqrt{\text{mW}}$.

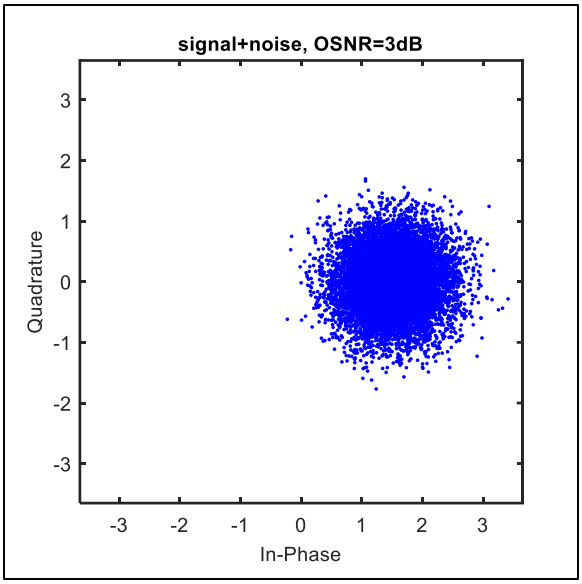

Fig. 15. Pulse amplitude distribution of averaged pule power 0 dBm, OSNR 3dB.

Now, after we have the series of amplitude, it's time calculate the bit error rate (BER). To calculate the BER, we need to define the decision area to decide each amplitude is an error or not. In the same case, 2-PAM using coherent detection, the signal can be $\{A_0, -A_0\}$. Thus, the decision area is simple, for the pulse with amplitude A_0, if the amplitude has real part less than zero $\text{real}(A'_{1\sim N}) < 0$, it will be regarded as an error, vice versa. The BER is the ration between the error bit number and total bit number. Here, my total bit number is 10^7, the BER in my calculation by using awgn() function is about 7.918×10^{-4}, BER by using wgn() function is about 8.072×10^{-4}. Further, the BER here is predictable. Base on the relation mentioned in section 2.3, the BER of 2-PAM signal using coherent detection can be represented as

$$BER_{2PAM,CD} = P_{e,2PAM,CD} = \Psi\left(\sqrt{\frac{2E_b}{N_0}}\right) = \frac{1}{2}\mathrm{erfc}\left(\sqrt{\frac{E_b}{N_0}}\right) \quad (18)$$

Due to the calculation above, we know that the $\frac{E_b}{N_0}$ here is 4.99, so the theoretical BER value here is $BER_{2PAM,CD} = 7.9284 \times 10^{-4}$. The simulation results above are in the same order.

Now, we can move on to an advanced modulated signal, 4-QAM. For the same averaged power, the amplitude of a 4-QAM signal can be $\{\frac{1+1i}{\sqrt{2}}A_0, \frac{-1+1i}{\sqrt{2}}A_0, \frac{-1-1i}{\sqrt{2}}A_0, \frac{1-1i}{\sqrt{2}}A_0\}$. If we have the same ASE noise power as the case above, $P_{ASE} = -3$ dBm $\cong 0.5$ mW, OSNR $= 3$ dB, the information SNR $= \frac{E_S}{N_0} \cong 4.99$. The amplitude distribution is in Fig. 16.

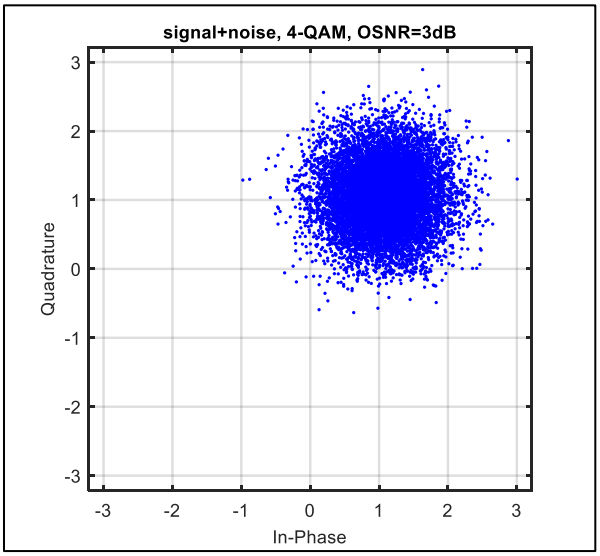

Fig. 16. Input pulse amplitude distribution of 4-QAM signal with averaged power 0dBm, OSNR 3dB.

The signal amplitude in this case is $\frac{1+1i}{\sqrt{2}}A_0$. Since the real and imaginary part of the amplitude are more close to zero, the error rate is higher than 2-PAM case although the noise power is the same. The symbol error rate here is $P_e \approx 0.0254$. The corresponding

BER is $BER_{QAM} \cong \frac{P_e}{log_2 M} \cong 0.0127$. On the theory side, the BER of M-QAM signal has form

$$BER_{M-QAM} \cong \frac{1}{log_2 M}\left\{1 - \left[1 - \frac{\sqrt{M}-1}{\sqrt{M}}\ erfc\left(\sqrt{\frac{3}{2(M-1)}\frac{E_{s,QAM}}{N_0}}\right)\right]^2\right\} \quad (19)$$

The theoretical BER value here is $BER_{4-QAM} \cong 0.0128$, the simulation value is very close to the theoretical value.

To sum up, we can see that with the same averaged signal power and the same noise power, if we choose to use 4-QAM modulation format, the BER is much higher than the 2-PAM format. In other words, 4-QAM signal is more sensitive to the noise, so the total transmission length should be shorter than the 2-PAM case to maintain the same BER performance.

3.2 Simulation result of the optical communication system

Base on the discussion in section 3.1, we can know the whole simulation process: create a series of initial pulse; let it propagate in some segments of fiber; after each segment of fiber, use an amplifier to compensate the fiber loss and add the ASE noise; calculate the BER performance at the receiver side. Here, we can have several different cases to study. First, no initial noise, only the ASE noise and the fiber dispersion and nonlinearity. We can compare the simulation result and the theory mentioned in section 2.3 to see if the

dispersion or the nonlinearity will affect the BER performance. Second, only the initial noise without fiber propagation, find the relation between the initial noise and BER, which has been shown in section 3.1.3. In this case the result of the simulation (generate a series of pulse amplitude with particular noise power and calculate the BER of this series of amplitude) and the theory (mathematical relation between BER and information SNR $= \frac{E_b}{N_0}$) are matched. However, one can notice that in order to achieve the 8×10^{-4} BER of the 2-PAM signal with 3dB OSNR, the number of the pulse we need is about 10^7. Thus, we can imagine that, in the first case with no initial noise, based on the Fig. 6, OSNR versus number of the amplifier in the section 2.3, the OSNR is much higher than 3dB if we only consider the ASE noise, so the number of the pulse we need should be much higher than 10^7. Since I use my laptop to run the simulation, it's really hard for me to simulate the first case. It turns out the third case, propagation with initial noise. In the following I will choose a high initial noise in order to reduce the number of pulse we need, let it propagate in the system and calculate the bit error rate, then compare the result between simulation and theory.

3.2.1 Optical system with PAM signal

Before the simulation, we can use the mathematical relation between OSNR, BER and amplifier number to predict what we should see. Fig. 17 describe the ONSR and BER behavior during the propagation. The system parameter is: 2-PAM format, averaged input

power 0 dBm, initial OSNR 0dB, single span includes 80 km SMF, 12.4 km DCF, and two EDFA with same gain value 11.1 dB.

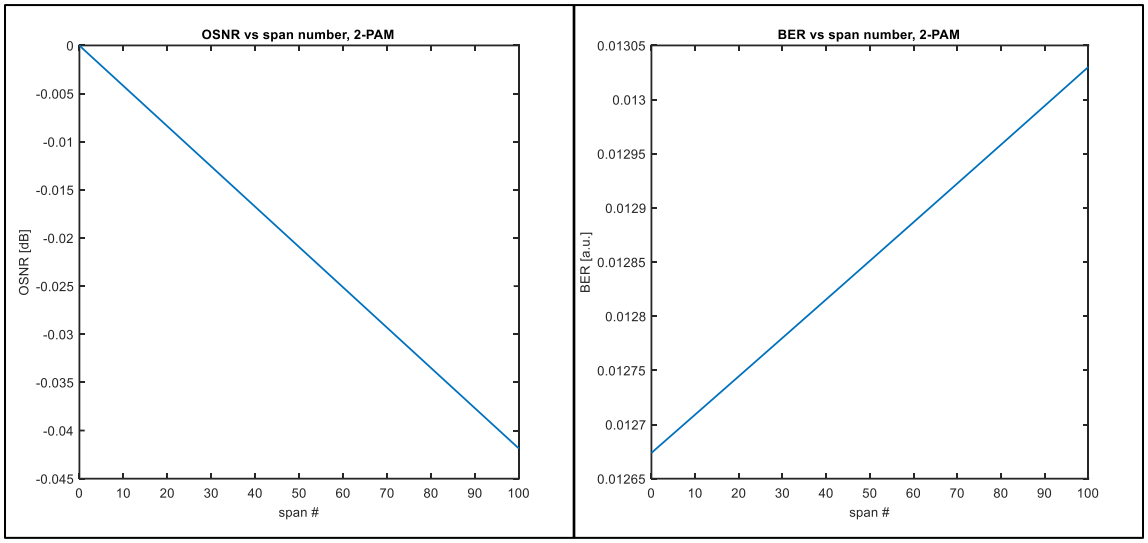

Fig. 17. OSNR and BER performance versus span number of 2-PAM signal

We can see that in this system, both OSNR and BER are changing very slowly. BER only increase 0.00035 after 100 spans in this system. Thus, we can imagine that the output signal should be similar to the input signal.

Fig. 18 is the simulation result of this system with 3 span propagation and using 6000 input pulses.

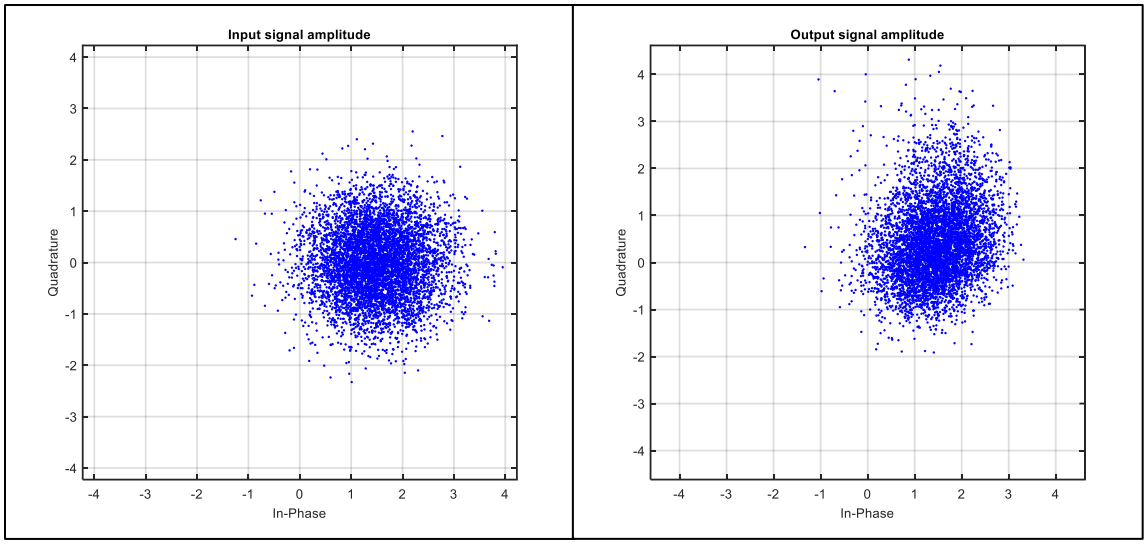

Fig. 18. Input and output amplitude distribution of 2-PAM signal.

It is interesting that the shape of the amplitude distribution is changed. The input signal has circle shape because the noise is Gaussian distribution, so as ASE noise. However, after this 3 span propagation, the output signal amplitude distribution is no longer circle. The in-phase part (real part) becomes small, and the quadrature part (imaginary part) becomes large. The BER increased from 0.0122 to 0.0155 ($\Delta\text{BER} = 0.0033$), higher than the prediction.

In order to know this shape change is caused by the propagation or not, we do some test. First, we close all the noise and let a series of the pulse with amplitude evenly distributed from 0 to 3 propagate in the system.

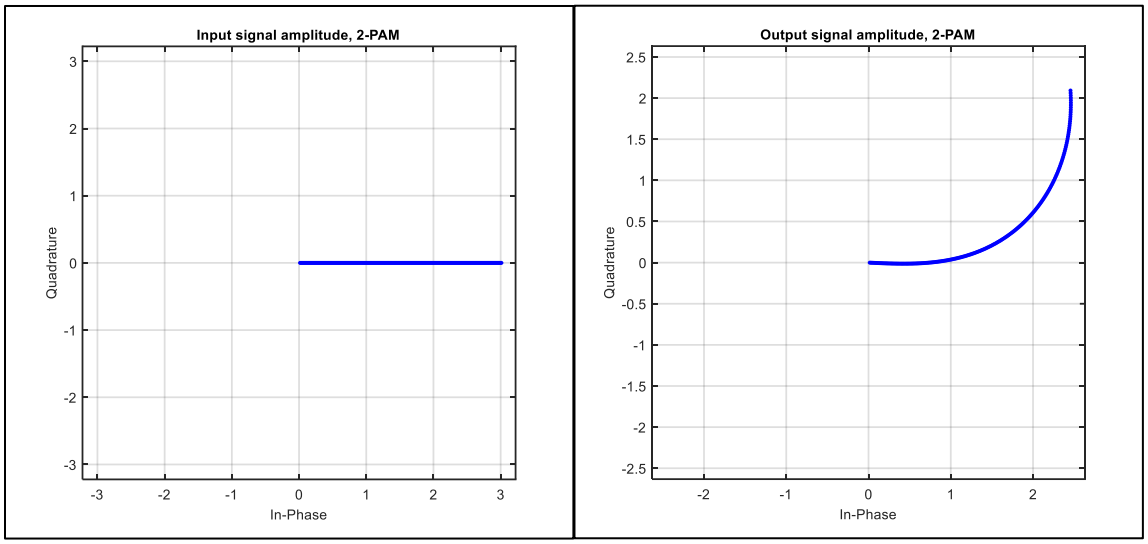

Fig. 19. Nonlinear phase shift of pulse amplitude.

As seen in Fig. 19, the pulse amplitude distribution is banding. The higher pulse amplitude has a larger phase shift. Compare to the output amplitude distribution above, the small amplitude maintains the same, and the high amplitude shift to a higher area, they are matched. Base on this property, we think that it is caused by the nonlinearity of the fiber because only the high amplitude has the phase shift. Thus, if we turn off the nonlinearity, set $\gamma_{SMF} = 0$ and $\gamma_{DCF} = 0$, the amplitude distribution should be the same.

We can observe from Fig. 20 that the output amplitude distribution maintains the circle shape as the input. The BER change from 0.0127 to 0.0121. The output BER is lower than the input BER, but I think it because the pulse number is not high enough. From the figure at the beginning of this section, the BER different of this 3 span system only consider the ASE noise is less than 0.00005. The number of the input pulse I use is 10000. Thus, the resolution of BER is 0.0001. This simulation result is not too strange.

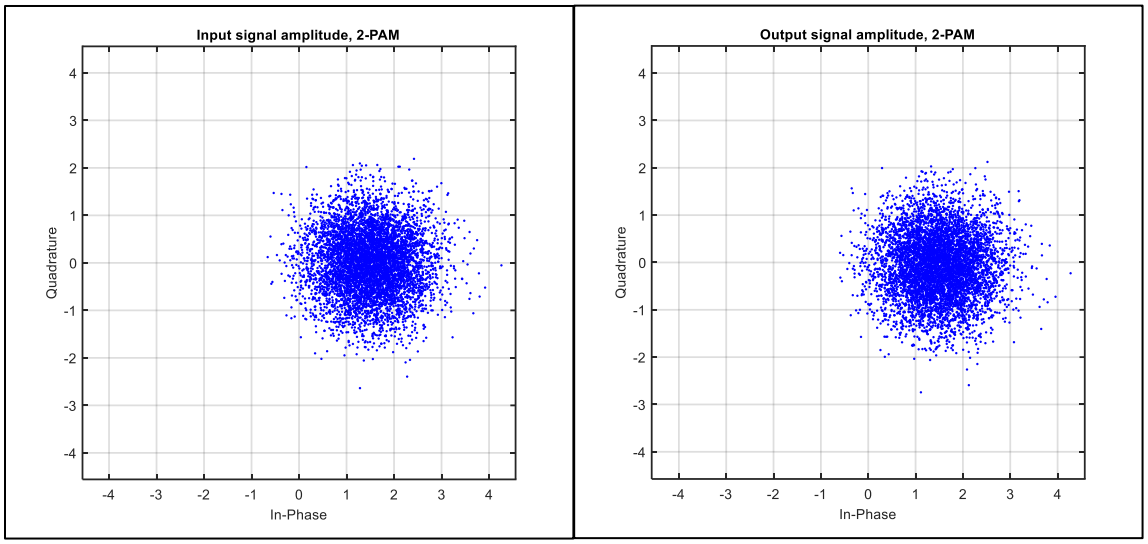

Fig. 20. Input and output amplitude distribution of 2-PAM signal, without nonlinearity.

Based on these tests, it is clear that the amplitude distribution shape-changing and the BER increase is due to the nonlinearity of the fiber. Now, the next question is how serious will the nonlinearity affect the BER performance of the system. From the test above we have seen that the BER increase 0.0033 during the 3 span propagation in the system with nonlinearity, and the BER doesn't increase without nonlinearity. But this is the performance of the signal with initial OSNR 0dB. For the practical situation, the transmitter modules produced by the industry nowadays usually have high initial OSNR about 50 dB. Almost all the pulse amplitude has the same value, and there is no high amplitude components which will see high nonlinear phase shift. The BER increase due to nonlinearity should be small. Unfortunately, it is really hard for me to simulate this extremely small initial OSNR. If I find a way to increase the efficiency of the code, I may have a chance to try this situation. However, there is still something we can try. The last test in this part is to see the accumulation of the nonlinear phase shift.

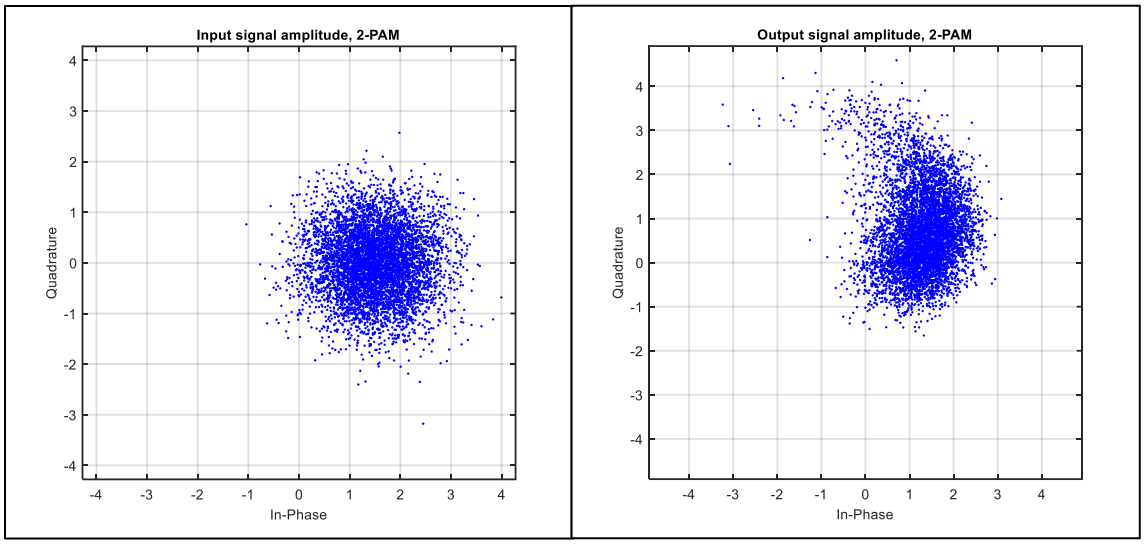

Fig. 21. Input and output amplitude distribution of 2-PAM signal, 6 spans.

In the previous test, the propagation length is 3 span. In Fig. 21, the propagation is 6 span. It is obvious that the banding becomes more serious. The BER increase from 0.013 to 0.0322 ($\Delta \mathrm{BER} = 0.0192$), much higher than the case with 3 span propagation (0.0033).

To sum up, from the simulation of this system we can learn that the nonlinearity affects the amplitude distribution of the signal and increase the BER. Further, this nonlinear phase shift will accumulate during the propagation, the longer propagation length of the system, the higher BER of the signal. On the other hand, it is a unique problem for the system using coherent detection. Since this nonlinearity only gives the signal a phase shift, but not change the power of it. The system using direct detection technique only detect the power of the signal, so nonlinear phase shift is not a problem. We can go back to see the theory in the section 3.1.2, the nonlinear part in the SSFM method is $\exp\left(\widehat{\mathrm{N}}\,\Delta \mathrm{z}\right) \mathrm{A}(\mathrm{z},\mathrm{t}) = \exp(i\gamma|A(z,t)|^2 \Delta \mathrm{z})\, \mathrm{A}(\mathrm{z},\mathrm{t})$, it put a time varying phase shift on the signal, but the absolute value of the signal maintain the same. In some research [10, 12, 25], this nonlinear phase shift effect is called common phase error. Since there signal has

high OSNR, every amplitude are really close to each other, every constellation point see the same phase shift, so it is “common” phase error. Further, they also have the solution for that [26]. The way they deal with this error is to use pilot tones inserted in the input signal. At the receiver side, by checking the phase of these pilot tones, one can know the rotation phase and correct the received signal. However, this solution only works for high OSNR. If the signal has low OSNR like the case here, the phase shift is no more “common.” We need to prevent the OSNR degraded to this low value while ASE noise accumulated during the propagation.

In the industry nowadays, it is not so popular for communication systems to use the coherent technique. But some company has produce transmitter modules using the coherent technique, like CFP2-ACO transceiver module. This module use modulation format from QPSK (4-QAM) to 16-QAM, producing highest 256 Gb/s for C-Band DWDM system, longest achievable transmission distance 2000 km. Since the requirement of transmission rate is growing, we can expect more coherent techniques developed in the future.

3.2.2 Optical system with QAM signal

In the simulation of the system with 2-PAM signal, we learn that the nonlinearity of the fiber affect the output signal amplitude distribution and increase the BER. We also see that this nonlinear phase shift will accumulate. Here, for the system with 4-QAM signal, we also start from the mathematical relation between OSNR, BER and span number without the considering of nonlinearity.

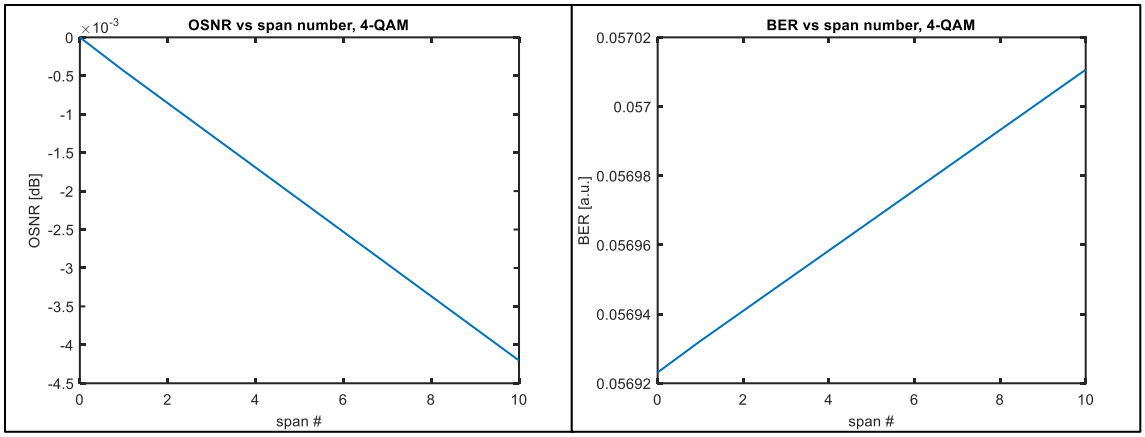

Fig. 22. OSNR and BER behavior of 4-QAM signal.

Since the distance between two constellation points of the 4-QAM signal ($\sqrt{2}A_0$) is smaller than that of 2-PAM signal ($2A_0$), the initial BER of 4-QAM signal is higher than 2-PAM signal with same OSNR, while the BER changing with span number is still very small without nonlinearity.

For the system with initial OSNR 0 dB, averaged input power 0 dBm, propagation length 3 spans. Fig. 23 is the input and output amplitude distribution and BER.

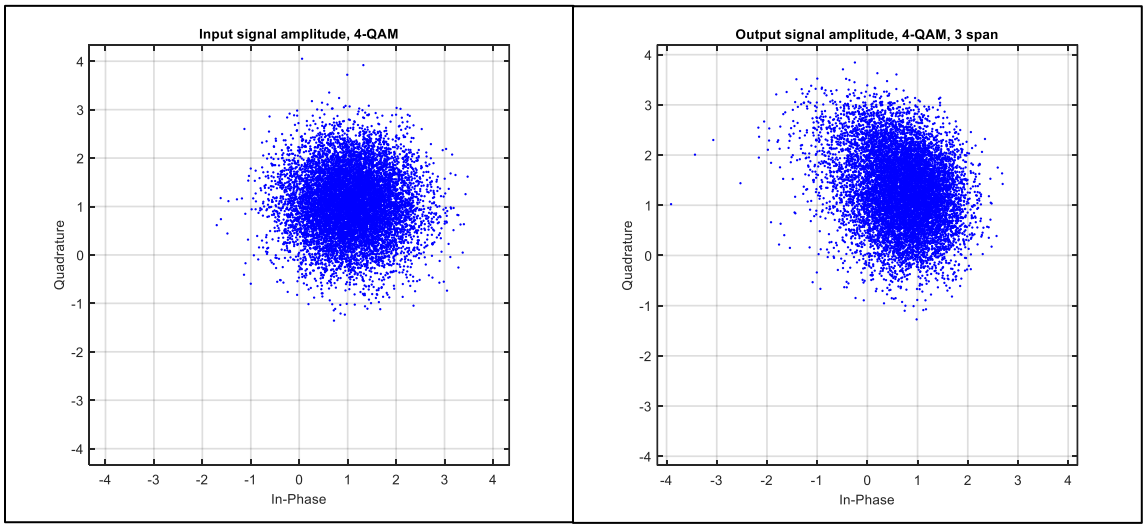

Fig. 23. Input and output amplitude distribution of 4-QAM signal, 3 span.

Just like the system with 2-PAM signal, we can see the amplitude distribution change and the BER increase from 0.0569 to 0.0854 ($\Delta BER = 0.0285$). Compare to the same propagation length and same initial OSNR case with the 2-PAM signal ($\Delta BER = 0.0033$); the 4-QAM system is more sensitive to the nonlinearity.

Since the QAM system has higher BER with initial OSNR 0dB, we can try to increase the initial OSNR to see the difference. The first try here is the simulation with initial OSNR 3dB.

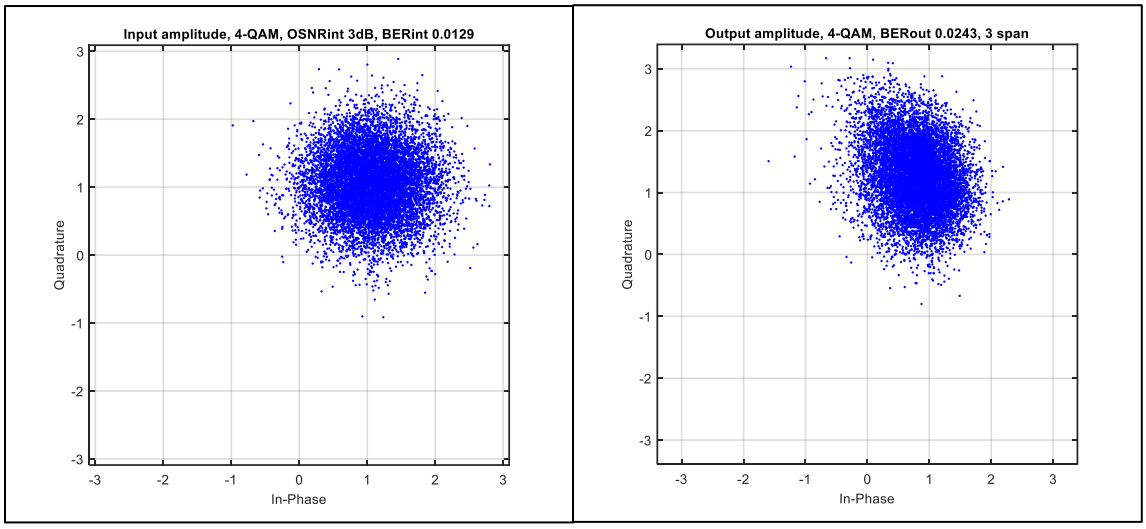

Fig. 24. Input and output amplitude distribution of 4-QAM signal, initial OSNR 3dB.

In Fig. 24, it shows that the BER increase from 0.0129 to 0.0243 ($\Delta BER = 0.0114$), which is smaller than the case with initial OSNR 0 dB ($\Delta BER = 0.0285$). One also can see from the figure that the shape-changing is slightly smaller than the case with initial OSNR 0 dB. This result is matched with the discussion in the 2-PAM system. The higher the initial OSNR, the lower the BER difference.

The last simulation is the change of the input power. The reason we choose the averaged input power to be 0 dBm is that it's the common choice in the industry. I had an

opportunity to tested several commercial transceiver modules this summer, and all of them have averaged power around 0 dBm. There are several reasons that I can think about it now. First one is power consumption, the higher power needs higher electrical power and higher cost. The second one is the trade-off between OSNR and nonlinearity. Base on the description of OSNR in section 2.3, $OSNR = \frac{P_{sig}}{P_{noise}} = \frac{P_{ch} - P_{sp,total}(\nu)}{P_{sp,total}(\nu)}$. Within the same noise power, if we have higher channel power, the OSNR can be higher and BER can be lower. However, due to the simulation result of the 2-PAM and 4-QAM system, the higher power will see more nonlinear phase shift and cause the error. Combine these consideration, we can do some simulation to check if 0 dBm is a good choice for the 4-QAM system. Previously, we already have the result with input power 0 dBm, initial OSNR 3dB, so the noise power here is -3 dBm. We can fix the noise power at -3 dBm and adjust the input power to -1 dBm and 1 dBm to see the BER changing.

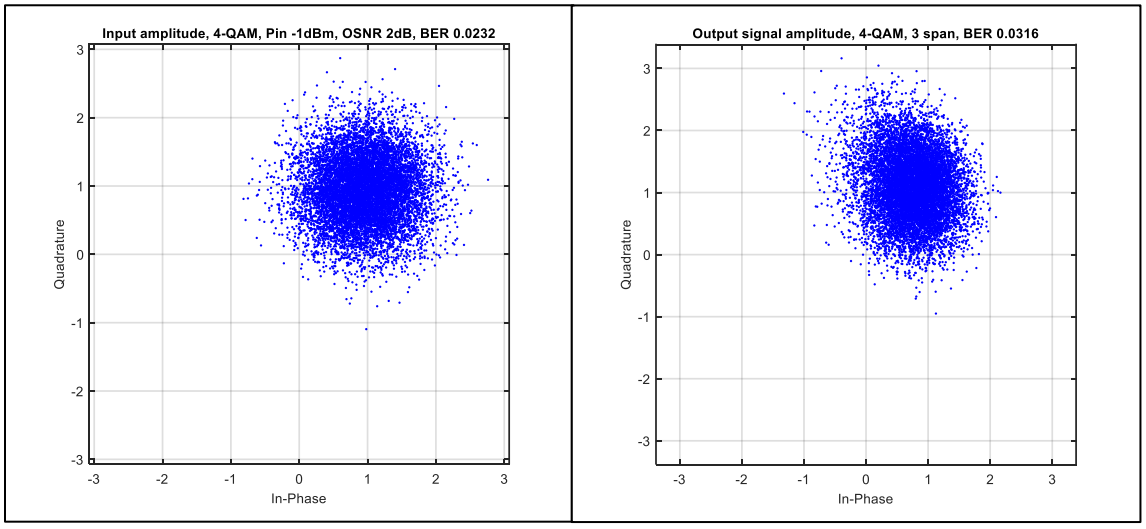

Fig. 25. Input and output amplitude distribution of 4-QAM signal, input power -1dBm.

Fig. 25 is the result of the input power -1 dBm, initial OSNR 2 dB case (so the noise power is -3 dBm). The BER increase from 0.0232 to 0.0316, $\Delta\text{BER} = 0.0084$. Compare

to the case of 0 dBm input power, this case has lower BER difference because the nonlinear phase shift is small, but the overall BER is higher due to the low initial OSNR. Thus, we can say that the OSNR induced BER is higher than nonlinearity induced BER in this case.

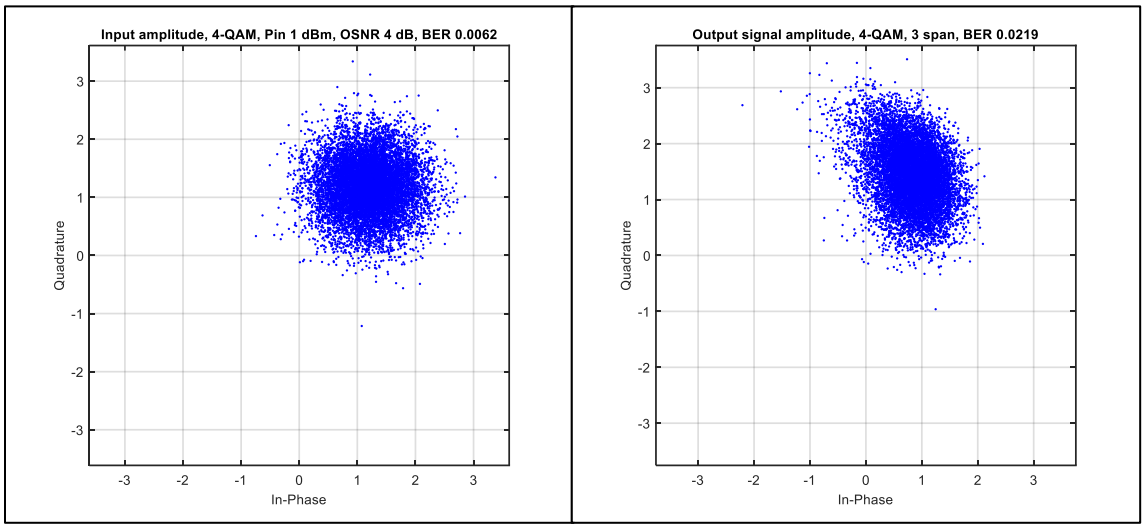

Fig. 26. Input and output amplitude distribution of 4-QAM signal, input power 1 dBm.

Fig. 26 is the case of input power 1 dBm and initial OSNR 4dB. The BER increase from 0.0062 to 0.0219 ($\Delta BER = 0.0157$). It is obvious that the shape change is large, and the nonlinearity induced BER is the largest among these three cases. However, due to the high initial OSNR and low initial BER, the output BER is still the lowest, slightly smaller than the case of 0 dBm input power. Base on the simulation results in this part, from the output BER point of view, we should choose the case of 1 dBm input power. If we want to cost down, we can also consider 0 dBm input power, since the overall BER performance is similar in these two cases.

Chapter 4

Conclusions

In this thesis, we study the impact of linear and nonlinear effects in optical systems with 2-PAM and 4-QAM signal. In Chapter 2, we study the theory about three main problems in the optical system and how we deal with them. Also, we introduce the mathematical relation between BER and parameters of the system. In Chapter 3, we investigate the process of solving nonlinear Schrodinger equation to simulate the evaluation of an optical pulse. After that, we show some simulation results of the BER performance of the system with 2-PAM and 4-QAM signal. Based on these results, it is obvious that the nonlinearity of the fiber changes the amplitude distribution shape and increase the BER of the system using coherent detection. Further, this nonlinear phase shift can accumulate, and the problem will become serious when we extend the propagation length. In the end, we study the BER performance versus different input power to see what is the optimized input power. So far, the simulation study here is limited by the efficiency of the code. In the future, if I can find some ways to increase the simulation speed, we can do some simulation with the situations more close to the industry level.

Reference

[1] Kao, K.C. and G.A. Hockham, *Dielectric-fibre surface waveguides for optical frequencies.* Proceedings of the Institution of Electrical Engineers-London, 1966. **113**(7): p. 1151-&.

[2] Xu, C., et al., *Comparison of return-to-zero differential phase-shift keying and on-off keying in long-haul dispersion managed transmission.* Ieee Photonics Technology Letters, 2003. **15**(4): p. 617-619.

[3] Szczerba, K., et al., *4-PAM for High-Speed Short-Range Optical Communications.* Journal of Optical Communications and Networking, 2012. **4**(11): p. 885-894.

[4] Ip, E., et al., *Coherent detection in optical fiber systems.* Optics Express, 2008. **16**(2): p. 753-791.

[5] Richter, T., et al., *Transmission of Single-Channel 16-QAM Data Signals at Terabaud Symbol Rates.* Journal of Lightwave Technology, 2012. **30**(4): p. 504-511.

[6] Winzer, P.J., et al., *Spectrally Efficient Long-Haul Optical Networking Using 112-Gb/s Polarization-Multiplexed 16-QAM.* Journal of Lightwave Technology, 2010. **28**(4): p. 547-556.

[7] Cai, J.X., et al., *Transmission of 96 x 100-Gb/s Bandwidth-Constrained PDM-RZ-QPSK Channels With 300% Spectral Efficiency Over 10610 km and 400% Spectral Efficiency Over 4370 km.* Journal of Lightwave Technology, 2011. **29**(4): p. 491-498.

[8] Winzer, P.J., *High-Spectral-Efficiency Optical Modulation Formats.* Journal of Lightwave Technology, 2012. **30**(24): p. 3824-3835.

[9] Richardson, D.J., J.M. Fini, and L.E. Nelson, *Space-division multiplexing in optical fibres.* Nature Photonics, 2013. **7**(5): p. 354-362.

[10] Armstrong, J., *OFDM for Optical Communications.* Journal of Lightwave Technology, 2009. **27**(1-4): p. 189-204.

[11] Cvijetic, N., *OFDM for Next-Generation Optical Access Networks.* Journal of Lightwave Technology, 2012. **30**(4): p. 384-398.

[12] Djordjevic, I.B. and B. Vasic, *Orthogonal frequency division multiplexing for high-speed optical transmission.* Optics Express, 2006. **14**(9): p. 3767-3775.

[13] Djordjevic, I.B., M. Cvijetic, and C.Y. Lin, *Multidimensional Signaling and Coding Enabling Multi-Tb/s Optical Transport and Networking Multidimensional aspects of coded modulation.* Ieee Signal Processing Magazine, 2014. **31**(2): p. 104-117.

[14] Fludger, C.R.S., et al., *1Tb/s Real-Time 4 x 40 Gbaud DP-16QAM Super-Channel Using CFP2-ACO Pluggable Modules Over 625 km of Standard Fiber.* Journal of Lightwave Technology, 2017. **35**(4): p. 949-954.

[15] Karanov, B., et al., *Span length and information rate optimisation in optical transmission systems using single-channel digital backpropagation.* Optics Express, 2017. **25**(21): p. 25353-25362.

[16] Essiambre, R.J., et al., *Capacity Limits of Optical Fiber Networks.* Journal of Lightwave Technology, 2010. **28**(4): p. 662-701.

[17] Cvijetic, M. and I.B. Djordjevic, *Advanced Optical Communication Systems and Networks*. Advanced Optical Communication Systems and Networks. 2013, Norwood: Artech House. 1-804.

[18] Ferreira, M.F., et al., *Polarization mode dispersion in high-speed optical communication systems.* Fiber and Integrated Optics, 2005. **24**(3-4): p. 261-285.

[19] Singh, S. and R.S. Kaler, *Analysis and minimization of cross phase modulation in semiconductor optical amplifiers for multichannel WDM optical communication systems.* Optics Communications, 2007. **274**(1): p. 105-115.

[20] Agrawal, G.P., *Nonlinear Fiber Optics*, in *Nonlinear Science at the Dawn of the 21st Century*, P.L. Christiansen, M.P. Sorensen, and A.C. Scott, Editors. 2000, Springer-Verlag Berlin: Berlin. p. 195-211.

[21] Kuschnerov, M., et al., *DSP for Coherent Single-Carrier Receivers.* Journal of Lightwave Technology, 2009. **27**(16): p. 3614-3622.

[22] Mu, R.M. and C.R. Menyuk, *Convergence of the chirped return-to-zero and dispersion managed soliton modulation formats in WDM systems.* Journal of Lightwave Technology, 2002. **20**(4): p. 608-617.

[23] Ladanyi, L., *Numerical studies of the nonlinear and dispersive propagation of optical pulses using the method of lines*, in *18th Czech-Polish-Slovak Optical Conference on Wave and Quantum Aspects of Contemporary Optics*, J. Perina, et al., Editors. 2012, Spie-Int Soc Optical Engineering: Bellingham.

[24] Sinkin, O.V., et al., *Optimization of the split-step Fourier method in modeling optical-fiber communications systems.* Journal of Lightwave Technology, 2003. **21**(1): p. 61-68.

[25] Armada, A.G., *Understanding the effects of phase noise in orthogonal frequency division multiplexing (OFDM).* Ieee Transactions on Broadcasting, 2001. **47**(2): p. 153-159.

[26] Jansen, S.L., et al., *Coherent optical 25.8-Gb/s OFDM transmission over 4160-km SSMAF.* Journal of Lightwave Technology, 2008. **26**(1-4): p. 6-15.